Does the hexosamine biosynthetic pathway play a role in mediating the beneficial effects of oleic acid in the heart?

Author: Miss ER Harris

Thesis presented for an MSc Degree

Faculty of Natural Science- Department of Physiological Science

Supervisor: Prof MF Essop

March 2012

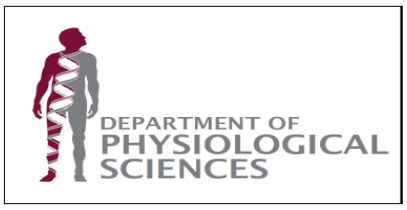

Declaration:

I understand what plagiarism is and I am aware of the University's policy in this regard.

I declare that this thesis is my own original work. Where other people have been used, this has been properly acknowledged and referenced in the accordance with departmental requirements.

I have not used work previously produced by another student or any other person to hand in as my own.

I have not allowed and will not allow anyone to copy my work with the intention of passing it off as his or her own work.

Signature: _____ Date: 30 February 12

Acknowledgements:

Firstly, I would like to thank the leader of my life-God, for giving me the courage, strength and the knowledge required to complete this degree. Without Him nothing is possible.

I would like to thank Prof Faadiel Essop, my supervisor, for guiding my project. It was challenging to be supervised by you. Most importantly, thank you for funding the first year of this degree (NRF), without the funding this project would not have been able to follow through.

Thank you to the DAAD organization for funding the second year of this degree, and for making the completion of this degree possible.

A very special thank you to Janola Harris, Pierre Harris, Ryan Harris, Alicia Harris and Peter Koeras for always encouraging me, supporting me and for listening & motivating me throughout my studying career. If I did not have all this support, I would not be where I am today. Thank you for your guidance and comforting words which really helped in times of immense pressure. To my parents thank you for taking care of me and pushing me to study further. To my siblings, thank you for the love, care and humorous moments that lit up my life. Thank you to Peter Koeras for being supportive, loving and always motivating me. I am grateful and blessed to have you all in my life.

I would also like to thank the following members of the Physiological Science Department:

- Dr. Benjamin Loos and Dr. Rob Smith for their help in analysing my cells and for training me on both the Flow cytometer and the Immunofluorescent microscope. I would also like to thank Dr. Rob Smith for answering random questions I had, and for trying his best to assist me as far as possible, even though he was in a different

research field. Thank you Dr. Rob Smith for setting the time aside to read and correct my thesis.

- Dr. Annadie Krygsman & Mr. Vuyo Mbovane for managing and maintaining the laboratories and making it possible to get work done.

- Catrina and Johnifer for keeping the laboratories a clean and sterile working environment.

- Dr. Theo Nell for managing the consumable orders and making sure that our materials arrive on time, as well as for always being willing to proof-read & correct my work. Thank you for always putting a smile on my face and building up a conversation whenever we meet in the department corridor. It meant a lot to me, and made me feel at home at times.

- The CMRG for assisting with techniques and giving valid input during presentation trial runs.

- Thank you to Prof Eugene Cloete (Dean: Science Faculty) for funding the completion year of my MSc.

Lastly, thank you to the University of Stellenbosch for granting me the opportunity to be a proud Matie and to be a part of the postgraduate research group in the Physiological Sciences Department.

Table of Contents

Abstract

Background:

Obesity is a growing global burden; current studies have projected the prevalence of obese / overweight individuals to increase to ~1.35 billion by 2030. A number of factors contribute to cardiovascular diseases, of which the focus of this study is what effect an increased level of free fatty acids has on the flux through the hexosamine biosynthetic pathway (HBP). It has been widely proven that an increased flux through the HBP causes an increase in protein *O*-GlcNAcylation, which leads to increased reactive oxygen species (ROS) production as well as an increase in cell death (apoptosis).

Methods:

For the purpose of this study a cell model was used. H9c2 cardiomyoblasts were cultured in 5ml Dulbecco's Modified Eagles Medium (DMEM) supplemented with 10% foetal bovine serum and 1% penicillin-streptomycin. The cells were then exposed to 0.25mM monounsaturated fatty acid (oleic acid) for 24, 48 and 72 hours respectively. The cultured cells were then evaluated to assess the degree ROS production, overall *O*-GlcNAcylation and cell death (apoptosis and necrosis), using flow cytometry and immunofluorescence microscopy.

Results:

We found that oleic acid causes a significant decrease in ROS production at the 48 hour time point when analysed on the flow cytometer, which indicates that oleic acid is

metabolized by the cells in a independent manner. Oleic acid also caused a significant decrease in cell death at all the time intervals. With regard to the HBP, oleic acid activates this pathway but causes downstream cardioprotective effects that do not necessarily occur along this pathway.

Conclusion:

This study explored whether a monounsaturated fatty acid, oleic acid, is able to act as a novel cardioprotective agent. The *in vitro* data supports this concept and we showed that it is able to blunt oxidative stress and cell death. It was also found that although oleic acid activated the HBP, it did not mediate its protective effects via this pathway only.

Opsomming

Agtergrond:

Vetsug is ‘n groeiende wêreldlas; huidige studies voorspel dat die voorkoms van vetsugtige / oorgewig individue toe sal neem tot ~1.35 biljoen teen 2030. Alhoewel verskeie faktore tot kardiovaskulêre siektes bydra is die fokus van hierdie studie om die effek van verhoogde vryvetsuurvlakke op die fluks deur die heksosamienbiosintestiese weg (HBW) te ondersoek.

Dit is reeds bewys dat verhoogde fluks deur die HBW ‘n verhoging in proteïen *O*-GlcNAsilering lei, wat verder tot verhoogde reaktiewe suusrtofspesies (ROS) vorming aanleiding gee en ook seldood (apoptose) verhoog.

Metodes:

‘n Selmodel is vir die doel van hierdie studie gebruik. H9c2 kardiomioblaste is in 5ml Dulbecco’s Modified Eagles Medium (DMEM) gekweek en gesupplementeer met 10% fetale beesserum en 1% penisillien-streptomysien. Die selle is blootgestel aan ‘n 0.25mM mono onversadigde vetsuur (oleïensuur) vir 24, 48 en 72 uur onderskeidelik. Die gekweekte selle is gevolglik ondersoek vir die graad van ROS ontwikkeling, algehele *O*-GlcNAsilering en seldood (apoptosis en nekrose), deur van vloeisitometrie en immunofluoresensie mikroskopie gebruik te maak.

Resultate:

Ons het bevind dat oleïensuur ‘n betekenisvolle verlaging in ROS ontwikkeling teen 48 uur soos bepaal deur die vloeisitometer, veroorsaak. Dit wys daarop dat oleïensuur deur die selle

op ‘n onafhanklike wyse gemetaboliseer is. Oleïensuur het ook ‘n betekenisvolle verlaging in seldood by alle tydsintervalle veroorsaak. Met betrekking tot die HBW het oleïensuur hierdie weg geaktiveer maar afstroom kardiobeskermings effekte versoorsaak wat nie noodwendig langs hierdie weg onstaan nie.

Gevolgtrekking:

Hierdie studie het die moontlikheid van ‘n mono-onversadige vetsuur, oleïensuur, om op te tree as ‘n nuwe kardiobeskermingsmiddel ondersoek. Die *in vitro* data ondersteun hierdie konsep en hier is aangetoon dat dit wel oksidatiewe stres en seldood onderdruk. Daar is verder bevind dat alhoewel oleïensuur die HBW aktiveer dit nie die beskermings effekte alleenlik via hierdie weg medieer nie.

List of Abbreviations

ACBP	Acyl-CoA binding protein
ACC	Acetyl CoA carboxylase
AGE	Advanced glycation end product
ARA	Arachidonic acid
ATP	Adenosine triphosphate
BAD	Bcl-2-associated death promoter
CAD	Coronary artery disease
CHD	Coronary heart disease
CPT-1	Carnitine palmitoyl transferase-1
CVD	Cardiovascular disease
DAPI	4'-6' diamidino-2-phenylindole
DHA	Docosahexaenoic acid
DMEM	Dulbecco's modified eagles medium
DON	6-diazo 5-oxo-L-norleucine
EGR-1	Early response growth factor 1
EPA	Eicosapentaenoic acid
ERK	Extracellular signal-regulated kinase
FABP	Fatty acid binding protein
$FADH_2$	Flavin adenine dinucleotide
FAT	Fatty acid translocase
FATP	Fatty acid transport proteins
FFA	Free fatty acids
FITC	Fluorescent isothiocyanate

FSC	Forward scatter
GAPDH	Glyceraldehyde-3-phosphate dehydrogenase
GFAT	Glutamine:fructose-6-phosphate amidotransferase
GlcN	Glucosamine
GLUT	Glucose transporter
HBP	Hexosamine biosynthetic pathway
HDL	High-density lipoproteins
IRS-1	Insulin receptor substrate-1
JNK	c-Jun NH_2-terminal kinase
LCFA	Long-chain fatty acid
LDL	Low-density lipoproteins
MAPK	Mitogen-activated protein kinase
MCD	Malonyl CoA decarboxylase
NADH	Nicotinamide adenine dinucleotide
OA	Oleic acid
O-GlcNAc	*O*-linked N-acetyl glucosamine
OGT	*O*-GlcNAc transferase
PARP	Poly-(ADP-ribose) polymerase
PBS	Phosphate buffered saline
PDH	Pyruvate dehydrogenase
PFK	Phosphofructose-1-kinase
PI3K	Phosphatidylinositol 3 kinase
PKB	Protein kinase B
PKC	Protein kinase C

RLU	Relative luciferase units
ROI	Region of interest
ROS	Reactive oxygen species
SSC	Side scatter
TG	Triacylglycerol
TNF	Tumour necrosis factor
UDP-GlcNAc	Uridinediphosphoglucose-N-acetylglucosamine

List of Tables & Figures

List of Tables

List of Figures

Chapter 1: Introduction

1.1 Epidemiology

Obesity is a global growing burden; current studies project that the prevalence of overweight / obese individuals will increase to ~1.35 billion by 2030 [45]. Epidemiological studies demonstrate that causes for this burden include genetics; age; gender; ethnicity; income brackets; poverty; urbanization; stress; lack of physical exercise and poor dietary habits [99]. Moreover, genetic inheritance also contributes, albeit to a lesser extent [99].

Urbanization is a central player in this process since populations are moving from rural to urban areas where they search for better employment, housing and education. This causes a shift in dietary patterns and lifestyle changes, thereby increasing the prevalence of health risks, particularly obesity and associated diseases, e.g. diabetes and cardiovascular diseases (CVD) [99].

Modern-day, western diets are typically high in carbohydrates and saturated fats [3]. The link between high fat intake and the onset of CVD is well established. However, high carbohydrate intake has recently also been identified as a major concern in this regard. For example, Majane *et al* [54] found that the consumption of high sugar diets caused a ~10% increase in body weight that ultimately led to hypertension and thus a pre-disposition to CVD. This study therefore shows that poor nutritional intake choices ('junk food') can be linked to the onset of heart failure [32]. Here, excess nutrients e.g. sugars are proposed to trigger maladaptive signalling pathways that contribute to the onset of impaired contractile function.

Thus, greater focus has been placed on improved nutritional intake and higher levels of exercise to help blunt the challenge of obesity and associated conditions, e.g. CVD. For example, altered serum cholesterol levels are now strongly linked to coronary artery disease

(CAD). In an effort to aid improved nutrition, health guidelines were set by the American Heart Association which are also implemented in clinical trials, i.e. Mediterranean-style Step I diet [45]. In similar fashion other lifestyle changes, e.g. reduced tobacco intake and/or increased exercise helps attenuate the growing incidence of obesity, type 2 diabetes and CVD. However, despite these attempts cardio-metabolic diseases continue to increase, especially in developing countries. For example, it is projected that the incidence of diabetes (~171 million in 2000) will double by 2030 [99]. Moreover, it is proposed that there is a link between CVD, physical inactivity and unhealthy diets which are major contributing factors. We face enormous challenges to manage cardio-metabolic diseases since it will result in marked effects in economies and overall productivity and well-being. Greater emphasis should therefore be placed on understanding the underlying mechanisms responsible since this should lead to improved therapy to treat diabetes and CVD.

Since the focus of this thesis is on the effects of a fatty acid on the viability of heart cells, I will now contextualize my work by providing a brief synopsis of cardiac metabolism.

1.2 Metabolism of the heart

The mammalian heart utilizes a variety of fuel substrates to generate adequate adenosine triphosphate (ATP) to sustain its function. These include fatty acids, glucose, lactate and ketone bodies [14]. Cardiac fuel substrate utilization is a dynamic process where the heart can switch between glucose (fed state) and fatty acids (fasted state), as an energy source. During the fasted state, circulating free fatty acid levels are high and fatty acids become the main energy source. Post prandially, a high-fat meal leads to increased lipoprotein lipase that

converts triglycerides to free fatty acids (FFA) that can undergo mitochondrial fatty acid oxidation.

During the fed state, when circulating glucose and insulin levels are high, fatty acid levels are low, with fatty acid oxidation attenuated while glucose oxidation increases. Post prandial hyperglycaemia following a high carbohydrate meal leads to increased plasma glucose levels and insulin secretion from pancreatic β-cells that ensures glucose uptake by peripheral tissues such as skeletal muscle and the heart [31, 86].

Conversely, during the fasted state circulating glucose and insulin levels decrease and the organism enters a catabolic state. Thus, glucose uptake and metabolism decrease while circulating fatty acid levels rise. In parallel, fatty acid uptake increases leading to higher mitochondrial fatty acid oxidation rates. During exercise, lactate becomes the major energy source [6, 30] that results in down regulation of both glucose oxidation and fatty acid uptake. Finally, during starvation ketone bodies can also act as a significant energy source for the heart [29].

The switch between glucose and fatty acids as fuel sources during the fed and fasted state was first described by Randle *et al*. in 1963, and is popularly known as the glucose-fatty acid cycle or Randle cycle. [24, 75] Randle *et al.* [75] describes the fuel flux between glucose and fatty acids and proposed that glucose utilization is decreased under conditions of high fatty acid oxidation. Under these conditions the heart will preferentially utilize one fuel versus the other. The by-products of fatty acid oxidation, i.e. NADH and acetyl-CoA inhibit the rate-limiting step of glucose oxidation, i.e. pyruvate dehydrogenase (PDH) [76]. This leads to a decrease in mitochondrial glucose metabolism. Furthermore, increased citrate generated from

acetyl-CoA may also inhibit glycolysis and glucose uptake though inhibition of 6-phosphofructose-1-kinase (PFK) in the glycolytic pathway.

On the contrary, high glucose oxidation can decrease fatty acid oxidation. Increased acetyl-CoA can be converted to malonyl-CoA a potent inhibitor of carnitine palmitoyl transferase-1 (CPT-1), the rate-limiting enzyme responsible for mitochondrial fatty acid uptake. This process takes place throughout the day depending on nutritional intake and levels. A brief review of the major metabolic fuel substrates of the heart, i.e. glucose and fatty acid metabolism will now be discussed.

1.2.1 Glucose metabolism – a brief synopsis

Cardiac glucose uptake is controlled by membrane-bound molecules known as glucose transporters (GLUTs). There are two major GLUT isoforms in the heart, i.e. GLUT1 and GLUT4 [66]. GLUT1 is the foetal isoform and is also non-insulin responsive while GLUT4 is the major adult isoform and is insulin responsive. Upon insulin stimulation, GLUT4 vesicles are translocated to the sarcolemma, thereby resulting in glucose uptake [66, 87].

Insulin exerts its effects by binding to insulin receptors and more specifically to the external α-subunit of the insulin receptor, the internal β-subunit self-phosphorylates, leading to tyrosine phosphorylation. This results in increased insulin receptor substrate-1 (IRS-1) and downstream PI3-kinase and Akt activity, that ultimately results in translocation of GLUT4 vesicles to the sarcolemma to facilitate glucose uptake [23].

Insulin plays a critical role in nutrient regulation of the circulatory system, especially for glucose and amino acids. The major target tissues of insulin are muscles, liver, adipose tissue and the satiety centre within the hypothalamus. The satiety centre is a collection of neurons sending signals to the brain to control appetite [85]. Insulin, however, does not directly affect the nervous system since it binds to membrane-bound receptors on target cells as discussed.

Insulin and insulin-receptor molecules are endocytosed by the target cell, whereby the insulin is subsequently released from the insulin receptors, and broken down within the cell. The receptors are released and become membrane-bound again. If glucose is not metabolized immediately by the cell it is stored as glycogen in skeletal muscle, liver and other tissues, or converted to fat in adipose tissue.

Without insulin the ability of cells to take up glucose is minimal, resulting in insulin resistance. The regulation of blood glucose levels is partially dependent on insulin. Therefore, if inadequate insulin is available glucose levels can increase drastically, leading to hyperglycaemia which is also one of the pre-disposing factors that contribute to the onset of diabetes and CVD.

During glycolysis, glucose is converted to glucose-6-phosphate via hexokinase and to fructose-6-phosphate by glucose-6-phosphate isomerase. Fructose-6-phosphate is subsequently converted to fructose 1,6-bisphosphate by phosphofructokinase, a rate-limiting enzyme of glycolysis. The majority of fructose-6-phosphate continues to be metabolized in the glycolytic pathway, until its end product, pyruvate, is formed. Interestingly, a relatively smaller percentage (~1-3%) enters a nutrient sensing pathway- called the hexosamine biosynthetic pathway (HBP) (refer to Figure 1.1) [55, 78, 93].

Pyruvate is usually formed under aerobic conditions, while under anaerobic conditions, lactate is formed from pyruvate. During the second phase of glucose metabolism, pyruvate enters the mitochondrion and undergoes oxidative decarboxylation. This process is catalysed by PDH that is located within the inner mitochondrion. PDH activity is usually increased by catecholamines or by high glucose levels (during the fed state).

Conversely, it is inhibited by acetyl-CoA and $NADH_2$ and by products of elevated fatty acid oxidation rates. Acetyl-CoA and $NADH_2$ can enter the Krebs cycle while reducing equivalents (NADH and $FADH_2$) can enter the electron transport chain to generate ATP [14, 66].

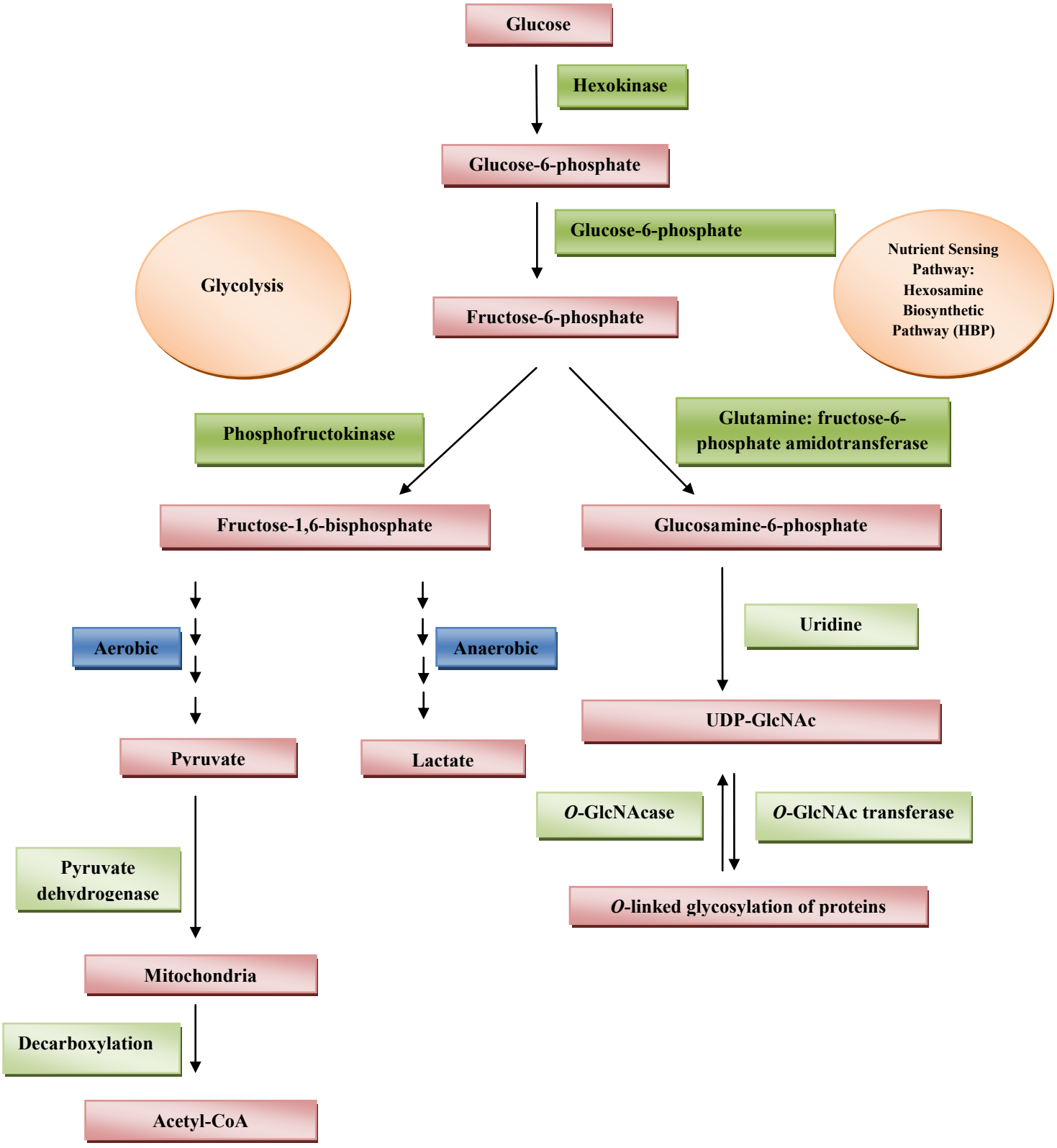

Fig 1.1: The relationship between glucose uptake and signalling pathways.

Glucose is one of the major fuel substrates in the heart during the fed state. Glucose, however, follows a series of reactions whereby the majority enters the glycolytic pathway and a smaller percentage feeds into the hexosamine biosynthetic pathway, which is a nutrient sensing pathway in the heart. The final product of the HBP, i.e. UDP-GlcNAc, can be *O*-linked to target proteins by *O*-GlcNAc transferase. Conversely, *O*-GlcNAcase can remove *O*-GlcNAc from target proteins.

Hyperglycaemia mediates tissue injury by generating reactive oxygen species (ROS) a mechanism well established by Brownlee *et al*. (2005). They propose that hyperglycaemia leads to increased glucose oxidation and flux through the electron transport chain rises. As a result there is greater mitochondrial superoxide production. Increased superoxide levels lead to DNA damage resulting in the activation of poly (ADP-ribose) polymerase (PARP). PARP can inhibit glyceraldehyde-3-phosphate dehydrogenase (GAPDH), a key enzyme of the glycolytic pathway [19]. The idea is then that such inhibition leads to the accumulation of upstream glycolytic metabolites, e.g. fructose-6-phosphate that can subsequently enter alternate metabolic pathways [2, 9, 11, 34-35, 37, 38, 55, 57, 75, 78, 80]. These include the production of advanced glycation end products (AGEs), increased flux through the HBP, polyol pathway and protein kinase C (PKC) activation [19].

1.2.1.1 Hexosamine biosynthetic pathway (HBP)

Since the focus of this thesis is on the HBP, I will now review the normal function of this pathway and also how dysregulated HP flux is linked to the onset of disease states, e.g. insulin resistance. Approximately 1-3% of available glucose enters into the HBP [77], where it is converted to glucose-6-phosphate with the aid of hexokinase, and then to fructose-6-phosphate via glucose-6-phosphate isomerase [55, 93]. Here, fructose-6-phosphate enters the HBP where it is then converted to glucosamine-6-phosphate via the addition of glucosamine (Figure 1.1).

HBP flux is regulated by glutamine: fructose-6-phosphate amidotransferase (GFAT), its rate-limiting enzyme. Intriguingly, GFAT overexpression causes insulin resistance, in parallel to increased HBP flux. Glucosamine-6-phosphate is converted to N-acetylglucosamine-6-phosphate by glucosamine-6-phosphate acetyltransferase, which is then converted to N-acetylglucosamine-1-phosphate by phosphate-acetylglucosamine mutase. The HBP end product is formed by the conversion of N-acetylglucosamine-1-phosphate to UDP-GlcNAc by the enzyme UDP-N-acetylglucosamine-pyrophosphorylase.

The final step of the pathway is the formation of uridine-diphosphate (UDP)-N-acetylglucosamine (GlcNAc) [55]. Many cytoplasmic and nuclear proteins are glycosylated on serine and/or threonine residues by the addition of a single *O*-linked-β-N-acetlyglucosamine (*O*-GlcNAc) molecule. Enzymes that are responsible for *O*-GlcNAc modifications are *O*-GlcNAc transferase (addition of *O*-GlcNAc) and *O*-GlcNAcase (removal of *O*-GlcNAc), which is preferentially cleaved by caspase 3. The role of the cleavage process is not known, although *O*-GlcNAcase is deregulated during programmed cell death (apoptosis) [98].

The *O*-glycosylation of proteins is implicated in protein modulation via different mechanisms that include *i) regulation of protein phosphorylation and protein function; ii) regulation of protein degradation; iii) protein localization; iv) protein-protein interaction modulation and v) mediating transcription* [78]. Data from *in vitro* studies done on RNA polymerase II showed a reciprocal relationship between *O*-GlcNAc and phosphorylation, where they compete for the same serine / threonine residues, thus regulating the levels of each other [12].

Although glucose is the main carbon source for HBP activation, fatty acids may also activate the HBP. Additionally, the HBP has been linked to both beneficial and detrimental effects. For the purpose of this study we focused on the effects that a beneficial monounsaturated fatty acid has on the HBP. Increased free fatty acids supply and β-oxidation increase the concentration of mitochondrial acetyl-CoA which decreases the rate of pyruvate oxidation via PDH inhibition [33]. The entry of fructose-6-phosphate into the glycolytic pathway is limited by the inhibition of phosphofructokinase (PFK) , thereby causing an elevated amount of fructose-6-phosphate to enter the HBP to form glucosamine (GlcN)-6-P and thus increased glycosylation of proteins via an increased formation of the HBP end product, UDP-GlcNAc [55, 93].

Increased flux of fructose-6-phosphate into the glucosamine pathway could lead to an impairment of glucose uptake due to the overload of substrate flowing into the HBP, which could ultimately lead to glucose-induced insulin resistance. Several studies have showed that an increased fructose-6-phosphate flux into the HBP causes decreased glucose uptake in both *in vivo* and *in vitro* studies which could lead to glucose- and fat-induced insulin resistance (Figure 1.2) [2, 9, 11, 34-35, 37, 38, 55, 57, 76, 79, 81].

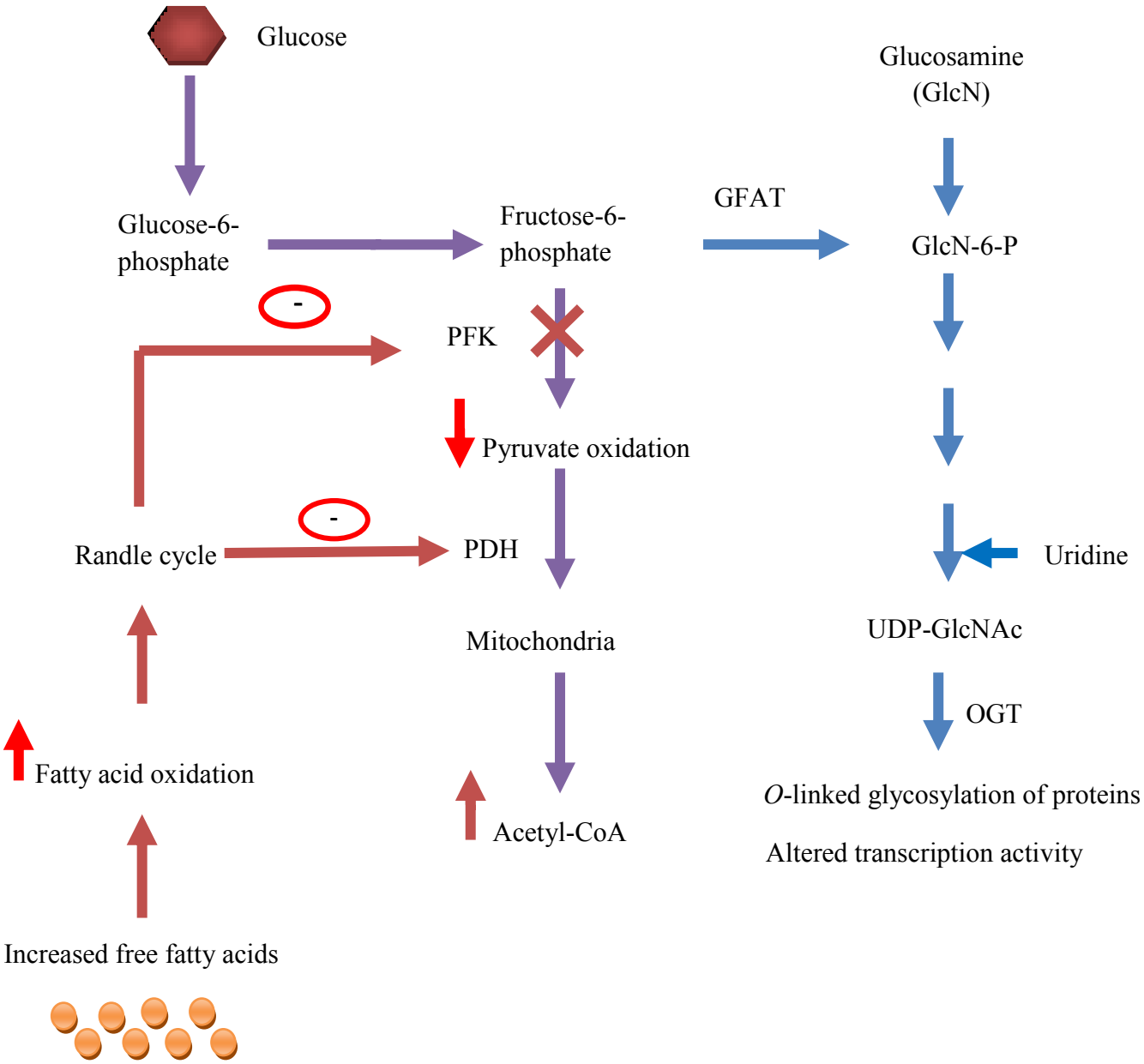

Fig 1.2 Fatty acids and the HBP.

An increase in the concentration of available free fatty acids leads to increased mitochondrial fatty acid oxidation. Due to the Randle effect PFK and PDH are inhibited resulting in an accumulation of upstream metabolites, i.e. fructose-6-phosphate. Thus, there will be increased HBP flux. Abbreviations: glutamine: fructose-6-phosphate (GFAT); *O*-GlcNAc transferase (OGT); pyruvate dehydrogenase (PDH); phosphofructokinase (PFK).

Essop *et al*., (2010) recently found, in response to increased glucose levels (hyperglycaemia), certain apoptotic proteins are *O*-GlcNAcylated [73, 74]. This was associated with higher oxidative stress and apoptosis in a heart cell line. Overall, our laboratory found that increased BAD *O*-GlcNAcylation results in less BAD becoming phosphorylated thereby causing more Bcl-2 proteins to dimerize with BAD, thus increasing Bax protein availability. Homodimerization of Bax causes the disruption of the mitochondrial membrane which leads to an increased number of cells becoming apoptotic [73, 74]. We also found that this pathway was induced in a rat model of diet-induced insulin resistance [73, 74].

However, others have found that an increase in *O*-Glycosylation can have cardioprotective effects. Chatham *et al*. (2010) found that glucosamine improved the cardiac functional recovery following an ischemic insult that was linked to increased *O*-Glycosylation [8]. It was further established that ERK1/2 and Akt responses were not altered by glucosamine; but merely attenuated the ischemic-induced increase in p38 phosphorylation. Thus, proposed that *O*-GlcNAcylation plays an important role as an internal stress response regulator, and such cardioprotection may involve the p38 MAPK pathway [26].

These studies therefore show conflicting outcomes when HBP is activated and further studies are required to resolve this. However, we are of the opinion that these outcomes depend on the particular intracellular context, i.e. acute vs. chronic and postulated that within the acute setting, specific proteins are targeted for *O*-GlcNAcylation, leading to cardioprotection. However, with chronic HBP activation, different proteins are targeted for *O*-GlcNAcylation, thus leading to detrimental outcomes, such as increased oxidative stress and apoptosis. These possibilities are currently being investigated in our group.

1.2.2 Fatty acid metabolism

Fatty acids are an important energy source for mammals and compromises ~80% of oxidative metabolism in humans [5, 15, 24, 49-51, 72]. Fatty acids have four important functions in the human body: i) they are the building blocks of phospholipids and glycolipids which constitute the cell membrane; ii) they are attached to proteins, which assist in directing them to their correct place within membranes; iii) are stored as triacylglycerols and iv) fatty acids and its products function as messenger molecules [90] and act on pancreatic β-cells, thus regulating glucose-stimulated insulin secretion [31, 86].

Long-chain fatty acids (LCFAs) provide 70-80% of the energy to sustain the heart's function [87, 97]. LCFAs are transported into the myocardium via protein-mediated LCFA transporters where uptake and oxidation is controlled by specific LCFA binding proteins which play an important role in LCFA movement across cellular membranes. The controlled movement of LCFAs into the cardiac myocytes contributes to the regulation of LCFA metabolism in healthy hearts.

Excess LCFAs (e.g. obesity, diabetes), contributes to the accumulation of toxic lipid metabolites (lipotoxicity) as well as glucose accumulation due to a lack of insulin responsiveness (glucotoxicity), which are associated with excess substrate accumulation in the heart [10, 71, 80, 91]. Several LCFA transporters are expressed in the heart, including an 88-kDa fatty acid translocase (FAT)/CD36, plasma membrane associated fatty acid binding proteins (FABP) and fatty acid transport proteins (FATP) [5, 51, 72].

Circulating free fatty acids (FFAs) are released into the bloodstream where they are then transported across the sarcolemma and into cardiomyocytes via mitochondrial membrane transporters. They are subsequently transferred to heart-type fatty acid-binding proteins (H-

FABP). It has recently been shown that one of the LCFA transporters, FATP1, displays acyl-CoA synthetase activity.

Following uptake, long-chain acyl-CoAs are complexed with acyl-CoA binding proteins (ACBP) (Figure 1.3) that can be transported to mitochondria for β-oxidation (70-80%). Alternatively, fatty acyl-CoAs can be esterified (10-30%) for triacylglycerol (TG) formation. Lipotoxicity is the result of a mismatch between lipid oxidation and lipid uptake [10, 71].

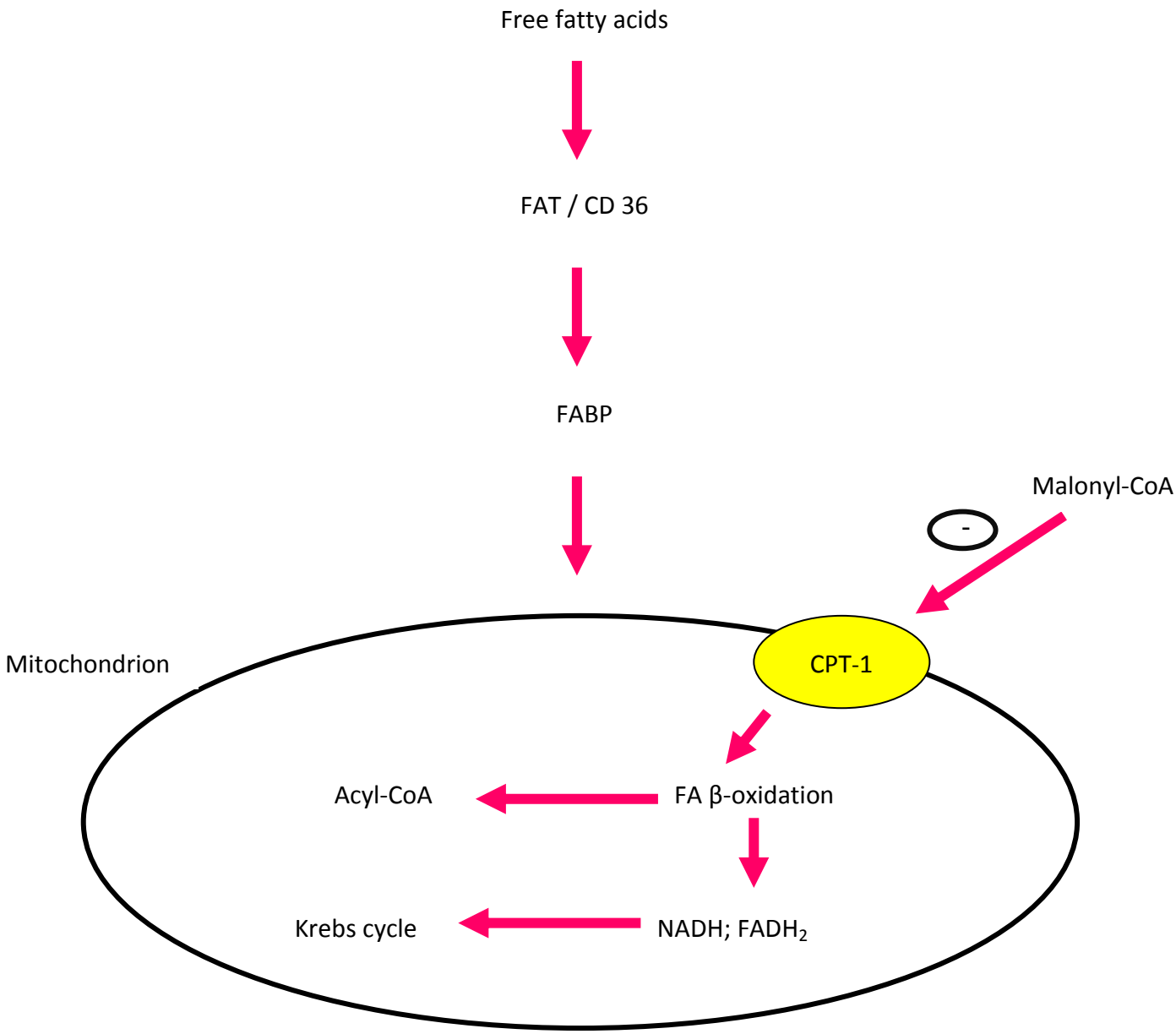

Fig 1.3 Schematic representation of protein-mediated, long-chain fatty acid uptake and its metabolism in cardiomyoblasts.

FAT/CD36 - fatty acid translocase; FABP - fatty acid-binding protein; FATP - fatty acid transport protein; ACBP - acyl-CoA binding protein; FA – fatty acids

Fatty acids are activated by the addition of coenzyme-A (catalysed by long-chain acyl Coenzyme-A synthase) after which mitochondrial uptake follows. The regulation of fatty acid metabolism is achieved by a series of reactions, involving the transport of fatty acids into the inner matrix of the mitochondrion where fatty acids are oxidized. Mitochondrial fatty acid

uptake is regulated by the rate-limiting enzyme CPT-1. CPT-1 is controlled by malonyl-CoA, a potent inhibitor [46-47, 65, 77, 82-83, 88, 101].

Upstream, acetyl-CoA carboxylase (ACC) synthesizes malonyl-CoA (from acetyl-CoA), while malonyl-CoA decarboxylase (MCD) can degrade malonyl-CoA [34-36, 39, 42, 43]. Thus, ACC and MCD activity can tightly regulate intracellular malonyl-CoA levels and mitochondrial fatty acid uptake [22].

Following mitochondrial uptake, fatty acids are catabolized via β-oxidation to ultimately generate reducing equivalents (NADH, $FADH_2$) that can enter the electron transport chain for ATP production [66].

A short review of the different types of fats and potential beneficial effects will follow with the main focus on oleic acid.

1.2.2.1 Unsaturated versus saturated fatty acids

A fatty acid is a carboxylic acid with a long unbranched carbon chain. Fatty acids are classed into three groups namely, monounsaturated, polyunsaturated and saturated fatty acids. Unsaturated fatty acids resemble saturated fatty acids, except its chain possesses one or more double bonds between the carbon atoms. Adjacent double-bonded carbons are in the *cis*-configuration, while double-bonded carbons situated across each other are in the *trans*-configuration. This configuration is important since fatty acid fluidity is affected in a restricted environment [1, 17, 95, 97].

Biological active fats are categorized as ‘good fats’ (comprising monounsaturated and polyunsaturated fatty acids), and ‘bad fats’ (comprising saturated and trans fatty acids) [52,

70, 92]. Broadly speaking, unsaturated fatty acids are enriched in fruits, vegetables, nuts and seeds, whereas saturated and trans fatty acids are typically found in meat, dairy products, refined oils and processed foods [52, 70, 92].

Saturated fatty acids are generally solid at room temperature. High intake of saturated fatty acids causes elevated cholesterol levels that lead to increased production of low-density lipoproteins (LDL). When LDL is present in excess, it can result in blocked arteries that may lead to atherosclerosis [56].

Trans fatty acids are detrimental to overall well-being. Like saturated fats, trans fats can also cause an increase in LDL levels, thus increasing the risk of CVD [56]. Moreover, in line with global trends, trans fats are often used in processed and packaged foods, as it increases the shelf-life of these foods.

Conversely, mono- and polyunsaturated fatty acids can reduce LDL and cholesterol levels [56]. The Mediterranean diet is a well know source of high monounsaturated fatty acid content and is linked with lower incidences of coronary heart disease (CHD) [56]., It has also been shown that the long-chain dietary polyunsaturated fatty acids, eicosapentaenoic acid (EPA) and arachidonic acid (ARA) protected neonatal rat cardiomyocytes from the damaging effects of simulated ischemia and reperfusion [21].

The latter two fatty acids decreased apoptosis through activation of extracellular signal-regulated kinase (ERK) and by de-phosphorylation of the pro-apoptotic kinase, p38 [21]. Mackay and Mochly-Rosen also found that ARA exerts its protective effects by selectively activating protein kinase C delta and epsilon (PKCδ, PKCε) [53] In agreement, long-term EPA and docosahexaenoic (DHA) treatment protected rat heart cells from hypoxia-reoxygenation injury [36]. Unsaturated fatty acids are recommended by dieticians as they

reduce the amount of calories compared to saturated and trans fatty acids. The following section will focus on studies that investigated the protective effects of oleic acid.

1.2.2.2 ***Oleic acid***

One of the major monounsaturated fatty acids is oleic acid (18:1ω9), an omega-9 fatty acid having 18 carbon atoms and a *cis* double bond at carbon 9 (Small, 2000). Sources of these fatty acids can be found in animal and vegetable oils such as olive oil and also grape seed and sea buckthorn oils. Stearoyl-CoA desaturase (SCD) catalyzes the biosynthesis of monounsaturated fatty acids from saturated fatty acids with preferred substrates including palmitoyl- and stearoyl-CoA, which are then converted into palmitoleoyl- and oleoyl-CoA, respectively [68]. Thus oleate can also be produced by palmitate metabolism. However, excess palmitate is known to have damaging effects, e.g. resulting in increased myocardial apoptosis [61]. Interestingly, low levels of oleate treatment was able to blunt detrimental effects of palmitate in heart cells [61]. Although palmitate has damaging effects in the heart, this may be undone by increased metabolism of oleate which has cardio-beneficial effects. Oleic acid has the ability to assist in certain beneficial functions such as reducing the development of atherosclerosis; decreasing serum cholesterol; diminishing oxidative stress and inflammatory mediators, and delaying the onset of adrenoleukodystrophy [62].

Omega-9 fatty acids reduce risk factors that contribute to CVD and diabetes, i.e. increase HDL cholesterol and to reduce LDL cholesterol, thus eliminating plaque formation in the arteries [56]. Due to high unsaturated fatty acid content, omega-9 fatty acids also reduce the risk of CAD [56].

Omega-3 fatty acids are known to have anti-inflammatory properties, while omega-6 fatty acids may have pro-inflammatory properties [27]. However, the effect of omega-9 on inflammation is not clear yet, although a number of studies have found that a high monounsaturated Mediterranean diet and / or consumption of olive oil can reduce inflammation [16, 40, 42, 45, 56, 67, 94].

Oleic acid also has the ability to activate PKC which in turn activates ERK [28, 44, 48, 63, 84]. ERK activation is a marker for cell growth and differentiation in response to several mitogens [18, 41]. A recent study also found that oleic acid has the ability to reverse the inhibitory effects of insulin production of the inflammatory cytokine (TNF-α). Oleic acid influenced expression of 14 genes, e.g. transcription factors such as the early response growth factor (EGR-1), ubiquitin and proteins involved in proteolysis. Interestingly, oleic acid is able to inhibit palmitate-induced oxidative stress, stress-associated protein kinases (p38, ERK1/2, JNK) and apoptosis in cardiac myocytes [61].

Although omega 3 and 9 fats are linked to cardioprotection (at population level) there are, as far as we are aware, no detailed heart studies done to determine cellular mechanisms whereby oleic acid could trigger cardioprotection. This served as a point of origin to investigate whether oleic acid possesses any anti-oxidant and / or anti-apoptotic properties that may explain its link to cardioprotection.

Together this literature review shows that various metabolic fuels (e.g. fatty acids and glucose) are required for optimal output by the mammalian heart. The regulation of fuel substrate supply is tightly controlled at multiple levels e.g. hormonal, cellular uptake, metabolic flux, gene, protein regulation, enzyme activity level, post-translational modification etc. Thus the organism needs to integrate a variety of signals at any instance to

ensure optimal fuel substrate selection and its breakdown to supply mitochondrial ATP to sustain the heart. The host organism is therefore finely tuned to achieve this balance or ‘’homeostasis’’.

However, on some occasions homeostatic balance cannot be restored, e.g. due to chronic factors (external or internal) that impact on the heart and the organism. In such instances, there may be a deficient or oversupply of metabolic fuels in the bloodstream and this in turn will determine the heart’s choices for substrate selection. Under these circumstances the heart may utilize an excess of an available fuel substrate, e.g. chronic fatty acid utilization by the diabetic heart. This in turn may eventually impair contractile function.

1.3 Hypothesis

As discussed earlier, excess fat and/or carbohydrate intake results in homeostatic imbalance. For example, in our laboratory we propose that elevated blood glucose levels (hyperglycemia) are damaging to the heart and results in cardiac contractile dysfunction. Here we propose that increased HBP flux results in greater *O*-GlcNAc modified signalling proteins that may eventually trigger oxidative stress and myocardial death. However, elevated HBP flux may also lead to cardio-protection – dependent on the particular context – and for the current study we therefore hypothesized that increased oleic acid availability will enhance HBP flux either directly or indirectly through alternative (but associated) pathways. This in turn will post-translationally modify different target proteins (increased protein *O*-GlcNAcylation), and thereby diminish oxidative stress and myocardial apoptosis, thus acting as a novel cardio-protective agent.

1.4 Aims

The aims of this study were three fold:

1. To evaluate whether oleic acid treatment increases HBP flux in H9c2 myoblasts

2. To determine whether oleic acid-induced HBP activation results in decreased oxidative stress; and lastly

3. To assess whether oleic acid-induced HBP activation results in attenuated myocardial apoptosis.

Chapter 2: Materials and Methods

2.1 Origin of H9c2 cardiomyoblasts

We employed rat-derived cardiovascular H9c2 cells for our *in vitro* studies. Kimes *et al*. (1976) [2] initiated the H9c2 cell line derived from an embryonic rat heart, and which is a useful cell line to simulate heart studies. Hescheler and co-workers (1991) [1] found that H9c2 cells have dihydropyridine-sensitive calcium channels that respond to beta-adrenergic stimulation. During rapid proliferation, calcium channels are sparse or absent, though at least two distinct potassium channels and a non-specific cation channel are observed [4]. The latter conduct calcium, sodium and potassium with similar efficacy.

2.2 Cell culture: H9c2 cardiomyoblasts

The H9c2 cardiomyoblast cell model was employed for the present study. Rat-derived H9c2 cardiomyoblasts were cultured in a T75 culture flask at a density of 10^6 cells/15 ml of low glucose Dulbecco's Modified Eagles Medium (DMEM) (Sigma-Aldrich, Steinheim, Germany). The DMEM was supplemented with 10% foetal bovine serum (Invitrogen, Carlsbad, CA) and 1% penicillin-streptomycin (Sigma, Steinheim, Germany) to reduce contamination. Cells were incubated overnight at a temperature of 37^{o}C, 95% air and 5% CO_2. The following day the medium was changed to discard all non-adherent cells. Subsequently, the adherent cells were further cultured in fresh medium and left to grow to between 70-80% confluence, where after cells were sub-cultured for further experiments. We ensured that the medium was regularly checked and replaced, since increased confluency depletes nutrients that may cause cells to detach from the flask surface and die.

2.3 Experimental protocol

After reaching 70-80% confluence, cells were sub-cultured. The cells were washed with 3 ml phosphate buffered saline (PBS) and thereafter treated with 4 ml trypsin (Sigma, Steinheim, Germany). This was followed by ~ 2 minutes incubation at room temperature to allow for cells to detach from the surface of the culture flask. Subsequently, 8 ml of fresh DMEM (Sigma, Steinheim, Germany) was added to the flask, bringing the total volume to 12 ml. After the contents were aspirated, 10 µl was transferred onto a hemocyter (Marienfeld, Germany) for counting. The remainder of the cell suspension was centrifuged (Orto Alresa, Digicen 20-R) for 3 minutes at 1,500 x g at 37°C. The supernatant was discarded and the pellet re-suspended in fresh DMEM according to the volume calculated from the 10 µl of cells that was used for counting (refer Appendix 1). Using this suspension, 250,000 cells / 5 ml DMEM (Sigma, Steinheim, Germany) were cultured in a T25 culture flask. The cells were incubated overnight at 37°C, 5% CO_2 and 95% air. The following day the medium was discarded, fresh medium added and cells were again incubated overnight.

We initiated our treatment protocol on the third day. Our strategy included the use of 0.25 mM oleic acid (OA) (Sigma, Steinheim, Germany) [5] and 40 µM DON (Sigma, St. Louis, MO) [3] that were added at different times to ensure that we adhered to our protocol (refer to Fig 2.1). Three time points, i.e. 24, 48 and 72 hour exposure time to OA (Sigma, Steinheim, Germany) were followed. The OA used to treat the cells was metabolised by the cells bound to albumin, in an undiluted form. To assess the effect of the hexosamine biosynthetic pathway (HBP) on our experimental system, we employed DON (GFAT inhibitor) (Sigma, St. Louis, MO) that was added 12 hours before the conclusion of the experiment (refer to Fig 2.1). DON was initially administered closer to the time that the cells were analysed (5-6 hrs).

However, since only minor changes were observed, we doubled exposure time to DON to allow for increased time for it to exert its known intracellular effects.

Upon completion of these experiments, we assessed various parameters to evaluate the validity of our hypothesis. Specifically, we determined the degree of oxidative stress; *O*-GlcNAcylation (HBP flux) and apoptosis by using flow cytometry as well as immunofluorescence microscopy (refer to Tables 2.1-2.2).

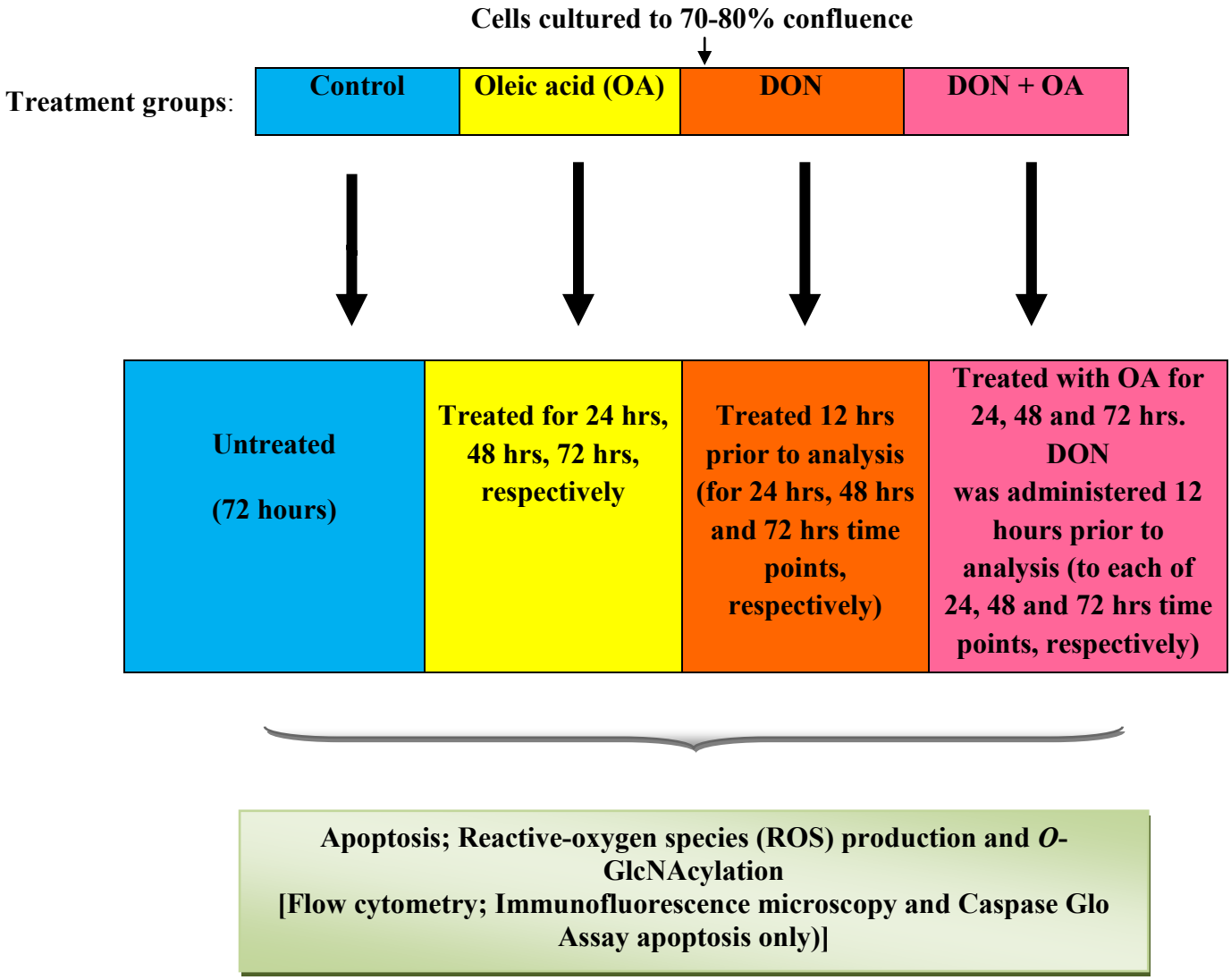

Fig 2.1 Overall experimental lay-out of this study

2.3.1 *Technique protocols*

<table>
<tr><th>Day</th><th colspan="3">FLOW CYTOMETRY
Experimental preparation: culture flasks</th></tr>
<tr><td>1</td><td colspan="3">250,000 (250 µl) cells from cell suspension (refer Section 2.3) were re-suspended in 5 ml DMEM in a T25 culture flask. The cells were incubated overnight at 37°C, 95% air and 5% CO_2 (10 flasks are prepared per experiment).</td></tr>
<tr><td>2</td><td colspan="3">Medium was discarded from all the flasks to remove non-adherent cells and fresh medium added. Cells were incubated overnight before treatment regimens were employed. The control flask remained untreated throughout the experiment.</td></tr>
<tr><td></td><td>0.25 mM Oleic Acid (OA)</td><td>40 µM DON</td><td>40 µM DON + 0.25 mM OA</td></tr>
<tr><td>3</td><td>378 µl OA into “72 hr flask”</td><td>No treatment</td><td>378 µl OA into “72 hr flask”</td></tr>
<tr><td>4</td><td>378 µl OA into “48 hr flask”</td><td>No treatment</td><td>378 µl OA into “48 hr flask”</td></tr>
<tr><td rowspan="2">5</td><td>378 µl OA into “24 hr flask”</td><td>No treatment</td><td>378 µl OA into “24 hr flask”</td></tr>
<tr><td>No treatment</td><td colspan="2">12 hrs prior to staining DON was administered where required (refer to Appendix 2 for calculations)</td></tr>
</table>

Table 2.1 Experimental design for the flow cytometry experiments.

<table>
<tr><th>Day</th><th colspan="3">IMMUNOFLUORESCENCE MICROSCOPY
Experimental preparation: 8-well LabTek chambers</th></tr>
<tr><td>1</td><td colspan="3">20,000 (20 µl) cells from the cell suspension (refer Section 2.3) were re-suspended in 500 µl DMEM per well. The cells were incubated overnight at 37°C, 95% air & 5% CO_2 (3 chambers were prepared per experiment).</td></tr>
<tr><td>2</td><td colspan="3">The medium was discarded from all wells to remove the non-adherent cells and replaced with fresh medium. Cells were incubated overnight before treatment. The control and PBS control wells remained untreated.</td></tr>
<tr><td></td><td>0.25 mM Oleic Acid (OA)</td><td>40 µM DON</td><td>40 µM DON + 0.25 mM OA</td></tr>
<tr><td>3</td><td>37.8 µl OA into “72 hr well”</td><td>No treatment</td><td>37.8 µl OA into “72 hr well”</td></tr>
<tr><td>4</td><td>37.8 µl OA into “48 hr well”</td><td>No treatment</td><td>37.8 µl OA into “48 hr well”</td></tr>
<tr><td rowspan="2">5</td><td>37.8 µl OA into “24 hr well”</td><td>No treatment</td><td>37.8 µl OA into “24 hr well”</td></tr>
<tr><td>No treatment</td><td colspan="2">12 hrs prior to staining DON was administered where required (refer to Appendix 2 for calculations)</td></tr>
</table>

Table 2.2 Experimental design for the immunofluorescence experiments.

2.4 Measurement of oxidative stress

2.4.1 Flow cytometry: H2DCF-DA staining

Cells were cultured as before to analyse cellular oxidative stress (refer Section 2.2 and 2.3). After the five-day experimental protocol (refer Table 2.1) was completed, the medium from all flasks was removed, cells were washed with 3 ml of warm PBS and thereafter treated with 4 ml trypsin (Sigma, Steinheim, Germany) for 2 minutes. After cell detachment, 8 ml DMEM (Sigma, Steinheim, Germany) was added to each flask. Following this, each flask's contents was transferred to a 50 ml plastic tube (Falcon) where after it was centrifuged (Orto Alresa, Digicen 20-R) at 1,200 x g for 20 seconds. The supernatant was discarded and pellets re-suspended in 200 µl H2DCF-DA dye which was calculated according to the supplier protocol (R&D Systems, Minneapolis, MD). A 1:200 dilution of ROS dye was prepared from a 1M stock solution by diluting it with sterile 1 x PBS. Flasks were incubated at 37°C for 10 minutes wrapped in foil.

Subsequently, the dye was aspirated and samples centrifuged (Orto Alresa, Digicen 20-R) at 1,200 x g for 20 seconds. The supernatants were discarded and the pellets were re-suspended in 300 µl warm PBS. The tubes were thereafter wrapped in foil and analysed using a BD FACSAria™ flow cytometer (Becton-Dickinson, CA) to evaluate oxidative stress.

The cell suspension was transferred from the 50 ml plastic tubes to specialized glass tubes for cytometric analysis. A total number of 5,000 – 10,000 events (cells) were collected per condition per experiment (each at different time points). This was a total of ~ 60,000 cells per experiment that was analysed, of which three independent experiments were conducted using the 488 nm laser; 520 LP and the 530/30 P emission filters were employed for the green signal (FITC colour channel was used).

The fluorescent intensity signal was measured by using the geometric mean on the intensity histogram for each condition. The geometric mean of each condition was then calculated in relation to the control (normalized) to evaluate the level of fluorescent intensity as a percentage across the time points, which was set equal to 100%. These intensity signals were used for statistical analysis. Intensity signals that were more than double the standard deviation were omitted. Each experiment was analysed independently (n=3).

The fluorescent peak of the H2DCF-DA dye (R&D Systems, Minneapolis, MD) on the histogram was used an indication of the overall degree of oxidative stress within the cell. A shift to the right indicated more oxidative stress in the selected events (number of cells analysed) whereas a shift to the left indicates less oxidative stress. The forward scatter (FSC) and the side scatter (SSC) on the system are indicators of the size of cells; the cells internal complexity as well as the fluorescence intensity (refer to Fig 2.2).

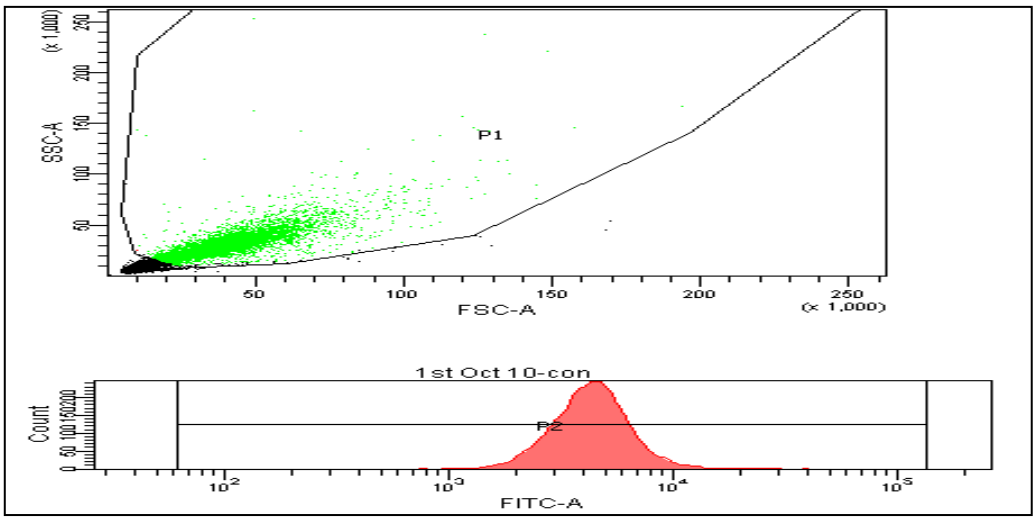

Fig 2.2 Flow cytometry fluorescent intensity histogram.

Here, P1 indicates all the events analysed; P2 indicates only the FITC-A positive events

2.4.2 Immunofluorescence microscopy: H2DCF-DA staining

Cells were cultured as before (refer Section 2.2 and 2.3) for the analysis of oxidative stress. After the 5-day experimental protocol (refer Table 2.2) was completed, the medium from all wells was removed, whereafter each well was washed with 300 µl warm PBS. PBS was subsequently removed and cells in each well re-suspended in 200 µl H2DCF-DA dye (R&D Systems, Minneapolis, MD). A 1:200 dilution of H2DCF-DA dye (R&D Systems, Minneapolis, MD) was prepared from a 1M stock solution by diluting it with sterile 1 x PBS. The chambers were incubated at 37°C for 10 minutes wrapped in foil.

Subsequently, the dye was aspirated and removed from each well. Wells were rinsed with 300 µl warm PBS and thereafter re-suspended in 200 µl Hoechst dye (Sigma, Steinheim, Germany) for 10 minutes. The dye was then removed and wells twice washed with 300 µl warm PBS. The chambers were wrapped in foil for the assessment of the degree of oxidative stress on the Olympus Cell^R system attached to an 1X-81 inverted fluorescence microscope (Olympus Biosystems, Germany) equipped with a F-view-II cooled CCD camera (Soft Imaging Systems, Germany).

Using a Xenon-Arc burner (Olympus Biosystems GMBH) as a light source, images were excited with the 360 nm, 472 nm or 572 nm excitation filter. Emission was collected using a UBG triple-bandpass emission filter cube. Each well was imaged individually using the 100x magnification on the oil immersion lens and Cell^R imaging software. Each experiment was imaged independently, where four images per well were taken per condition, thus having a total number of 16 images per time point and 40 images per experiment. In each image there were 10-20 cells that were imaged, thus a total number of 400-800 cells were imaged per experiment. Moreover, this experiment was repeated three times (independently).

Each image was background subtracted and the regions of interest (ROI) for each cell in a single image were selected for which the fluorescent intensity was automatically calculated by the Cell^R software and averaged. The average of each ROI per condition of cells imaged per time point was used for statistical analysis. Each experiment was analysed independently (n=3).

The fluorescent intensity of the H2DCF-DA dye (R&D Systems, Minneapolis, MD) was an indication of the degree of oxidative stress. The FITC colour filter was used, observed as a green fluorescent staining of the cell cytoplasm, to measure overall oxidative stress within the cell. The degree of green intensity reflected the degree of oxidative stress.

2.5 Evaluating the level of O-GlcNAcylation: an indication of HBP flux

2.5.1 Flow cytometry

Cells were cultured to measure the degree of *O*-GlcNAcylation (refer Section 2.2 and 2.3). After the 5-day experimental protocol (refer Table 2.1) was completed, medium was removed and each flask washed with 3 ml warm PBS. Thereafter, the cells in each flask were treated with 4 ml trypsin (Sigma, Steinheim, Germany) for 2 minutes to allow cells to detach from culture flask surfaces. After detachment, 8 ml DMEM (Sigma, Steinheim, Germany) was added to each flask, the cell suspension in each flask was then transferred to 50 ml plastic tubes and centrifuged (Orto Alresa, Digicen 20-R) for 20 seconds at 1,200 x g. Thereafter, the supernatant in each tube was discarded, and the pellets re-suspended in 300 µl cold PBS followed by centrifugation (20 seconds, 1,200 x g). The supernatant was discarded; pellets re-suspended in 300 µl of a 1:1 methanol/acetone fixative and incubated for 10 minutes at 4°C. Subsequently, samples were re-centrifuged (Orto Alresa, Digicen 20-R) (1,200 x g, 20

seconds) and the supernatant discarded. In the meantime, a 5% donkey serum in PBS (5 mL) stock solution was prepared and 200 µl added per flask to block non-specific binding sites. Samples were incubated for 10 minutes at room temperature, where after the supernatant was discarded (no centrifugation and no washing). A 1:200 dilution of primary anti-goat antibody (Pierecenet, Woburn, MA) in PBS stock solution was prepared. We added 100 µl from the stock solution to each tube, followed by incubation for 30 minutes in the dark at room temperature. Subsequently, the samples were centrifuged and the supernatants discarded. The pellets were washed with 300 µl cold PBS, re-centrifuged (Orto Alresa, Digicen 20-R) at 1,200 x g for 20 seconds and the supernatants discarded.

A 1:200 dilution of secondary anti-mouse PE-Texas Red antibody (Invitrogen, Carlsbad, CA) in PBS stock solution was then prepared, where after 100 µl was added to each tube and incubated for 30 minutes at room temperature in the dark. Following this, 100 µl of Hoechst dye (Sigma, Steinheim, Germany) (1:200 dilution in PBS) was added and incubated for 10 minutes at room temperature in the dark. All reagents and dyes should be kept on ice and in the dark throughout the staining procedure due to light sensitivity.

Samples were thereafter centrifuged (Orto Alresa, Digicen 20-R) at 1,200 x g for 20 seconds and the supernatants discarded. We then washed samples with 300 µl PBS, re-centrifuged (1,200 x g for 20 seconds) and added 300 µl PBS to the final pellet. Subsequently, samples were wrapped in foil while transporting it to a BD FACSAria™ Flow Cytometer (Becton-Dickinson, CA) for analysis.

Prior to analysis, the cell suspension was transferred from the 50 ml plastic tubes to specialized glass tubes for cytometric analysis. A total number of 5,000 – 10,000 events (cells) were collected per condition per experiment (each at different time points). This was a

total of ~ 60,000 cells per experiment that was analysed, of which three independent experiments were conducted using the 488 nm laser; 610 LP and the 616/23 BP emission filters were employed for the red signal (PE-Texas Red colour channel was used). The fluorescent intensity signal was measured by using the geometric mean on the intensity histogram for each condition.

The geometric mean of each condition was then calculated in relation to the control (normalized), to evaluate the level of fluorescent intensity as a percentage across the time points, which was set equal to 100%. These intensity signals were used for statistical analysis. Intensity signals that were more than 2x the standard deviation were omitted. Each experiment was analysed independently (n=3).

2.5.2 Immunofluorescence microscopy

Cells were cultured as before to assess the degree of *O*-GlcNAcylation by imaging (refer Section 2.2 and 2.3). After the five day experimental protocol (refer Table 2.2) was completed, the medium from all wells was removed using a vacuum pump. Each well was thereafter washed with 300 µl of warm PBS and cells fixed for 10 minutes at 4°C by using 300 µl of a 1:1 methanol/acetone fixative. Subsequently, the fixative was removed and wells left to air dry for 20 minutes. In the meantime, a 5% donkey serum in PBS (5 mL) stock solution was prepared, which was used in later steps of the staining process.

Thereafter, wells were washed with 300 µl cold PBS followed by the addition of 50 µl of 5% donkey serum to block non-specific binding sites. Samples were incubated for 20 minutes at room temperature, where after the serum was drained (no centrifuging and no washing) and a

1:200 dilution of primary antibody in PBS stock solution added (100 µl). Samples were thereafter incubated overnight wrapped in foil at 4°C.

The following day the primary antibody was drained using a vacuum pump and each well washed with 300 µl PBS. A 1:200 dilution of secondary anti-mouse Texas Red antibody (Invitrogen, Carlsbad, CA) in PBS stock solution was then prepared, of which 100 µl was added to each well and incubated for 30 minutes at room temperature in the dark. We thereafter added 100 µl of Hoechst dye (Sigma, Steinheim, Germany) (1:200 dilution in PBS) to each well and incubated for a further 10 minutes at room temperature in the dark. All reagents and dyes should be kept on ice and in the dark throughout the staining procedure due to light sensitivity. Wells were twice washed with 300 µl PBS to prevent cell dehydration.

The chambers were wrapped in foil while conveying it to an Olympus Biosystems Immunofluorescent Microscope (Olympus Biosystems, Germany) for cell imaging. The Olympus Cell^R system is attached to a 1X-81 inverted fluorescence microscope (Olympus Biosystems, Germany) equipped with an F-view-II cooled CCD camera (Soft Imaging Systems, Germany). Using a Xenon-Arc burner (Olympus Biosystems GMBH) as a light source, images were excited with the 360 nm, 472 nm or 572 nm excitation filter. Emission was collected using a UBG triple-bandpass emission filter cube.

Each well was imaged individually using the 100x magnification on the oil immersion lens and Cell^R imaging software. Each experiment was imaged independently, where four images per well were taken per condition, thus having a total number of 16 images per time point and 40 images per experiment. In each image there were 10-20 cells that were imaged, thus a total number of 400-800 cells were imaged per experiment. Moreover, this experiment was repeated three times (independently).Each image was background subtracted and the ROI for

each cell in a single image were selected for which the fluorescent intensity was automatically calculated by the Cell^R software and averaged. The average of each ROI per condition of cells imaged per time point was used for statistical analysis. Each experiment was analysed independently (n=3).

The level of *O*-GlcNAcylation can be observed by the fluorescent intensity of the Texas Red in the cytoplasm. The fluorescent intensity of the Texas Red dye (Invitrogen, Carlsbad, CA) was an indication of the degree of *O*-GlcNAcylation. The Texas Red filter was used, observed as a red fluorescent staining of the cell cytoplasm, which measured the protein *O*-GlcNAcylation within the cell. The more intense the red signal observed was, the more protein *O*-GlcNAcylation occurred, an indication of increased HBP flux.

2.6 Assessment of apoptosis & necrosis

2.6.1 Flow cytometry: Propidium iodide & Annexin V staining

Cells were cultured for apoptotic cell analysis (refer Section 2.2 and 2.3). After the five day experimental protocol (refer Table 2.1) was completed, DMEM (Sigma, Steinheim, Germany) in all flasks were discarded and cells washed with 3 ml of warm PBS. Thereafter, cells in each flask were treated with 4 ml of trypsin (Sigma, Steinheim, Germany) for two minutes to allow for detachment from the culture flask surface. After detachment, 8 ml DMEM (Sigma, Steinheim, Germany) was added to each flask.

The cell suspension in each flask was transferred to individual 50 ml tubes and centrifuged (Orto Alresa, Digicen 20-R) for 20 seconds at 1,200 x g at 37°C. Thereafter supernatants were discarded and pellets re-suspended in 500 µl cold $CaCl_2$ PBS (refer Appendix 3 for

calculation). The $CaCl_2$ PBS assists with the binding of the dye. The tubes were re-centrifuged (Orto Alresa, Digicen 20-R) at 1,200 x g for 20 seconds at 37°C.

Thereafter the supernatants were discarded and cell suspensions re-suspended in 100 µl 1x binding buffer (R&D Systems, Minneapolis, MD) followed by centrifugation (Orto Alresa, Digicen 20-R) for 20 seconds at 1,200 x g at 37°C. After discarding the supernatants, pellets in each tube were re-suspended in 100 µl binding buffer and 10 µl Annexin V dye (R&D Systems, Minneapolis, MD).

Samples were incubated for 15 minutes in the dark at room temperature and thereafter centrifuged (Orto Alresa, Digicen 20-R) at 1,200 x g for 20 seconds. After the supernatants were discarded, pellets were washed with 50 µl 1x binding buffer (R&D Systems, Minneapolis, MD) and re-centrifuged (Orto Alresa, Digicen 20-R) (1,200 x g for 20 seconds). After the supernatants were discarded, this step was repeated and final pellets were re-suspended in 5 µl propidium iodide dye (R&D Systems, Minneapolis, MD) and 100 µl 1x binding buffer (R&D Systems, Minneapolis, MD).

The cells were then immediately viewed on a BD FACSAria™ Flow Cytometer (Becton-Dickinson, CA). The early phase apoptotic cells were viewed in the fourth quadrant (Q4) (absorbed the Annexin V dye), the second quadrant (Q2) indicated cells that were necrotic (propidium iodide stained) and in the late apoptotic phase (Annexin V stained). Moreover, the first quadrant (Q1) represented only the necrotic cell population, and the third quadrant (Q3) indicated all the viable cells.(refer to Fig 2.3).

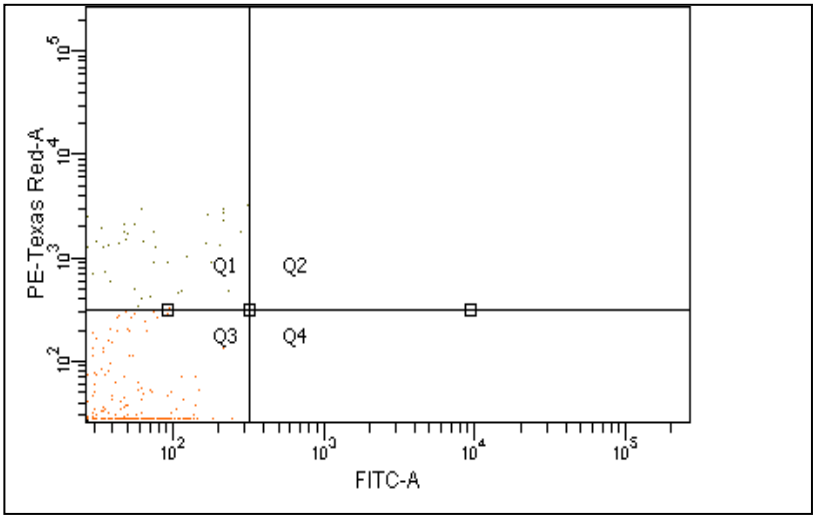

Fig 2.3. Flow cytometry quadrant lay-out.

The cell suspension was transferred from the 50 ml plastic tubes to specialized glass tubes for cytometric analysis. A total number of 5,000 – 10,000 events (cells) were collected per condition per experiment (each at different time points). This was a total of ~ 60,000 cells per experiment that was analysed, of which three independent experiments were conducted using the 488 nm laser; 520 LP and the 530/30 P emission filters were employed for the green signal (FITC colour channel was used). The fluorescent intensity signal was measured by using the cell number in each quadrant out of 100% of P1 (whole population analysed) on the intensity histogram for each condition.

The apoptotic / necrotic cell number of each condition was then calculated in relation to the control. These intensity signals were used for statistical analysis. Intensity signals that were more than 2x the standard deviation were omitted. Each experiment was analysed independently (n=3).

The fluorescent peak of the Annexin-V dye (R&D Systems, Minneapolis, MD) on the histogram was used as an indication of the number of apoptotic cells. A shift to the right

indicates more apoptosis in the selected events, whereas a shift to the left indicates less apoptosis. The forward scatter (FSC) and the side scatter (SSC) on the system are indicators of cell size and, internal complexity, as well as fluorescence intensity respectively.

2.6.2 Immunofluorescence microscopy: Hoechst staining

Cells were cultured and sub-cultured in preparation for apoptotic cell imaging (refer Section 2.2 and 2.3). After the 5-day experimental protocol (refer Table 2.2) was completed, the medium from all the wells were removed using a vacuum pump and each well was washed with 300 µl of warm PBS. Thereafter, 300 µl of a 1:1 methanol/acetone fixative was added to each well and incubated for 10 minutes at 4°C. After 10 minutes the fixative was removed and wells left to air dry for 20 minutes. In the meantime a 5% donkey serum in PBS (5mL) stock solution was prepared to block non-specific binding sites, which was used in later steps of the staining procedure.

After the wells had air dried, wells were washed with 300 µl PBS and 100 µl of Hoechst dye (Sigma, Steinheim, Germany) (1:200 dilution in PBS) added to each well. This was incubated for a further 10 minutes at room temperature in the dark. Thereafter, the contents in each well were removed, wells were washed twice with PBS, where after 300 µl PBS was added per well. The chambers were then wrapped in foil while transporting to the Olympus Biosystems™ Immunofluorescent Microscope (Olympus Biosystems, Germany) for imaging due to light sensitivity.

The Olympus Cell^R system is attached to a 1X-81 inverted fluorescence microscope (Olympus Biosystems, Germany) equipped with an F-view-II cooled CCD camera (Soft Imaging Systems, Germany). Using a Xenon-Arc burner (Olympus Biosystems GMBH) as a

light source, images were excited with the 360 nm, 472 nm or 572 nm excitation filter. Emission was collected using a UBG triple-bandpass emission filter cube.

Each well was imaged individually using the 40x objective lens and Cell^R imaging software. Each experiment was imaged independently, where four images per well were taken per condition, thus having a total number of 16 images per time point and 40 images per experiment. In each image there were 10-20 cells that were imaged, thus a total number of 400-800 cells were imaged per experiment. Moreover, this experiment was repeated three times (independently).Each image was background subtracted and the number of apoptotic cells in each image was selected and the average number of apoptotic cells was calculated per condition, which was used for statistical analysis. Intensity signals that were more than 2x the standard deviation were omitted.

Each experiment was analysed independently (n=3). Cells were counted as apoptotic based on nuclei condensation or fragmentation. The Hoechst (DAPI) filter was used, which was observed as a blue fluorescent staining of the cell nucleus, and employed a mechanism to assess cell death.

2.6.3 Caspase-Glo 3 assay

Cells were cultured for apoptotic cell analysis (refer Section 2.2 and 2.3). After the five day experimental protocol (refer Table 2.3) was completed, the medium in all the wells were discarded. The cells in each well were thereafter treated with 100 µl caspase assay reagent from the Caspase-Glo® 3/7 assay kit (Promega, Madison, WI) and incubated at room temperature for three hours. Thereafter the cells from each well were transferred to a white-walled 96-well luminometer plate (Amersham, Buckinghamshire, UK).

The white wall 96-well plate was then analysed in a luminometer (Glomax, 96 Micoplate Luminometer™). The caspase activity in each well was analysed to provide an indication of the degree of apoptosis. The number of apoptotic cells was calculated by the software on the computer that was linked to the luminometer.

The number of apoptotic cells were then used for statistical analysis. Intensity signals that were more than 2SD were omitted. Each experiment was analysed independently (n=3).

<table>
<tr><th>Day</th><th colspan="3">Experimental preparation: 96-well chambers</th></tr>
<tr><td>1</td><td colspan="3">20,000 cells (20 µl) from the cell suspension (refer Section 2.3) were re-suspended in 100 µl DMEM per well. Cells were incubated overnight at 37°C, 95% air and 5% CO_2.</td></tr>
<tr><td>2</td><td colspan="3">The medium was discarded to remove non-adherent cells and fresh medium was added to each well. Cells were subsequently incubated overnight before treatment. The control wells remained untreated.</td></tr>
<tr><td></td><td>0.25 mM Oleic Acid (OA)</td><td>40 µM DON</td><td>40 µM DON + 0.25 mM OA</td></tr>
<tr><td>3</td><td>7.56 µl OA into “72 hr wells”</td><td>No treatment</td><td>7.56 µl OA into “72 hr wells”</td></tr>
<tr><td>4</td><td>7.56 µl OA into “48 hr wells”</td><td>No treatment</td><td>7.56 µl OA into “48 hr wells”</td></tr>
<tr><td rowspan="2">5</td><td>7.56 µl OA into “24 hr wells”</td><td>No treatment</td><td>7.56 µl OA into “24 hr wells”</td></tr>
<tr><td>No treatment</td><td colspan="2">12 hrs prior to staining DON was administered where required (refer Appendix 2 for calculations)</td></tr>
</table>

Table 2.3 Experimental design for the caspase 3 assay.

2.7 Data analysis

Statistical analysis was performed using Graph Pad Prism 5. Results were expressed as a mean ± standard error of mean (SEM) of all experiments. Intergroup differences were analysed using non-parametric one-way analysis of variance (ANOVA) with the Newman-Keuls Multiple Comparison test for column analyses. Values were considered to be significant at $p<0.05$.

Chapter 3: Results

3.1 H9c2 cell culture conditions

H9c2 cardiomyoblasts were cultured in T25 culture flasks in low glucose medium and at three time intervals, i.e. 24, 48 and 72 hrs. Cells were also treated with oleic acid ± 6-diazo-5-oxo-L-norleucine (DON) (GFAT inhibitor). DON treatments were initiated 12 hours prior to analysis and would be expected to reduce HBP flux. This experimental protocol was followed to assess the degree of oxidative stress, HBP activation (*O*-GlcNAcylation) and cell death (apoptosis and necrosis).

3.2 Measurement of oxidative stress

Cells were initially analysed on a flow cytometer to measure the degree of oxidative stress. No significant differences were found following oleic acid treatment, except at the 48 hr time interval, although this decrease was not significant (Figure 3.1).

3.2.1 Flow cytometry: H2DCF-DA staining

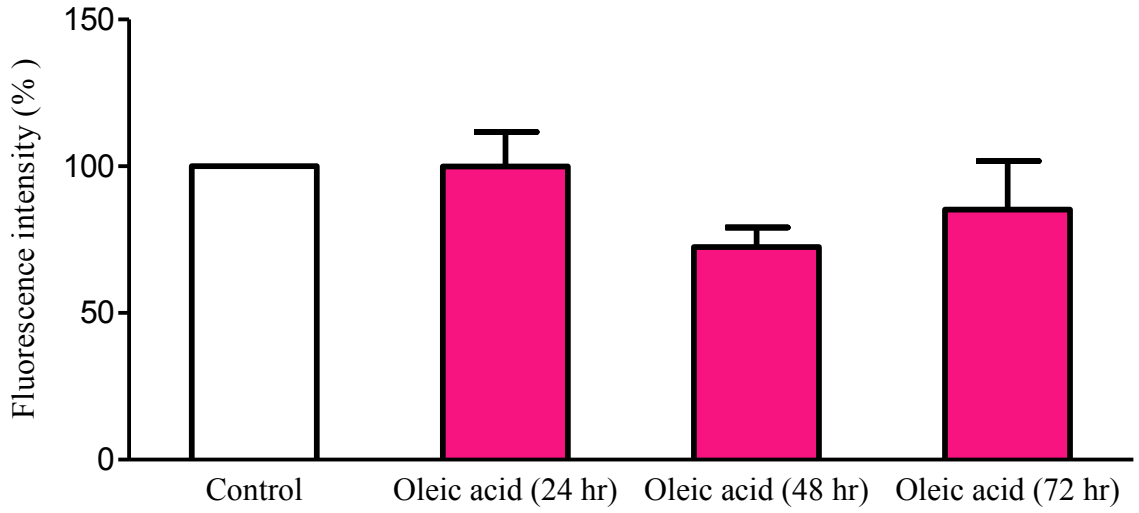

Fig 3.1 Evaluating the effects of oleic acid treatment on the degree of oxidative stress (flow cytometry)

H9c2 cardiomyoblasts were treated with 0.25 mM oleic acid for 24 hr, 48 hr and 72 hr, respectively. Cells were thereafter analysed on the flow cytometer to measure the degree of oxidative stress as described in the Materials and Methods section of this thesis (refer to section 2.4.1) – (n=3).

We next treated cells with an HBP inhibitor (DON) to determine the role of the HBP in this model under the same conditions. DON treatment decreased oxidative stress levels at 24 hours to 67.2 ± 9.6% in comparison to the control and at 48 hours to 72.2 ± 11.0% in comparison to the control ($n=3$, $p<0.05$), but not at the 72 hour time interval (Figure 3.2). Additionally, the sole treatment of oleic acid at 48 hours decreased oxidative stress to 73.8 ± 9.2% in comparison to the control, and the combined treatment of oleic acid and DON also decreased oxidative stress in the cells to 80.7 ± 4.9% in comparison to the control at 48 hours ($n=3$, $p<0.05$). However, no additive effect was observed for oleic acid and DON treatment.

I.

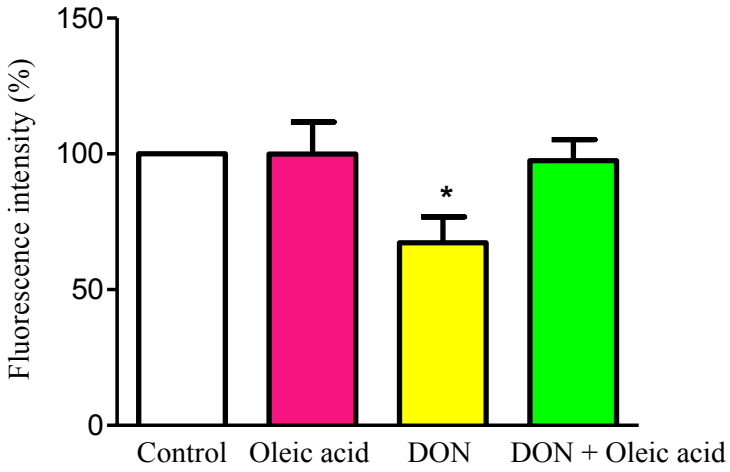

II.

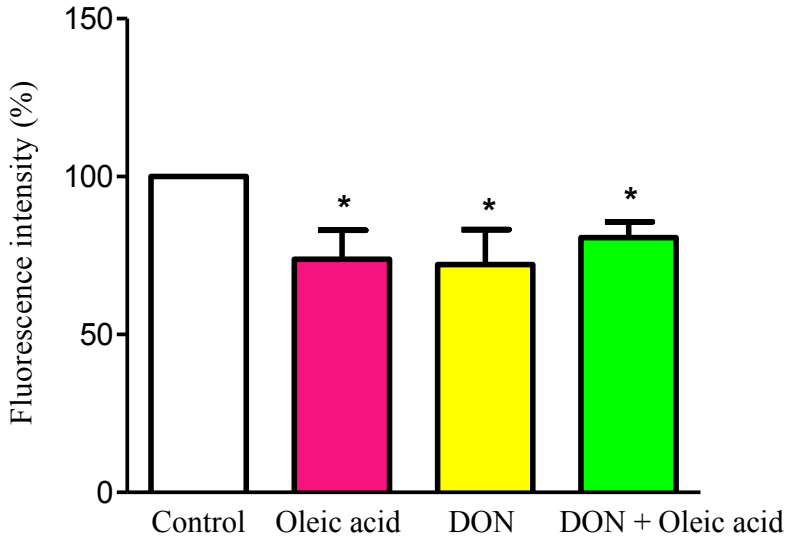

III.

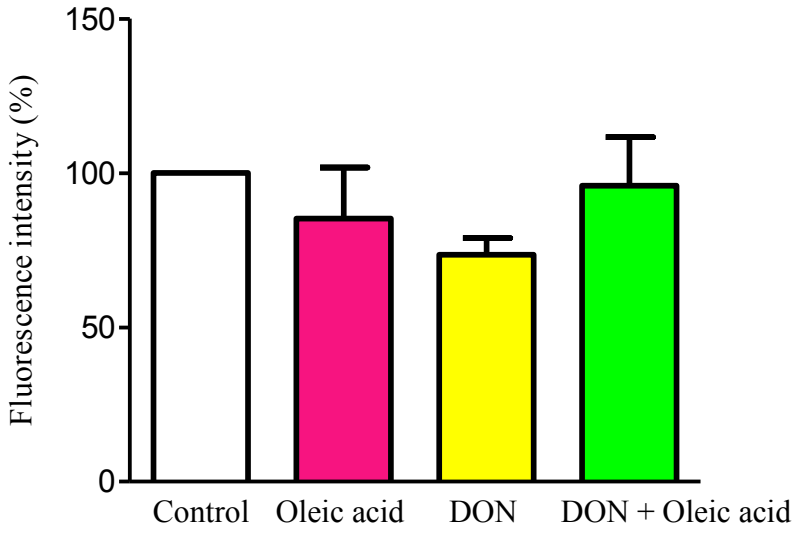

Fig 3.2 The effect of oleic acid treatment ± HBP inhibition on oxidative stress (flow cytometry)

H9c2 cells were treated with oleic acid ± DON for 24 hr (I), 48 hr (II) and 72 hr (III), respectively. Subsequently, cells were analysed on the flow cytometer to measure the degree of oxidative stress as described earlier (refer to section 2.4.1 of the Materials and Methods section of this thesis). * $p<0.05$ versus control. Values are expressed as mean ± SEM - (n=3).

3.2.2 Immunofluorescence microscopy: H2DCF-DA staining

To further confirm these findings we evaluated cells by immunofluorescence imaging. However, we found no significant changes with oleic acid treatment (Figure 3.3).

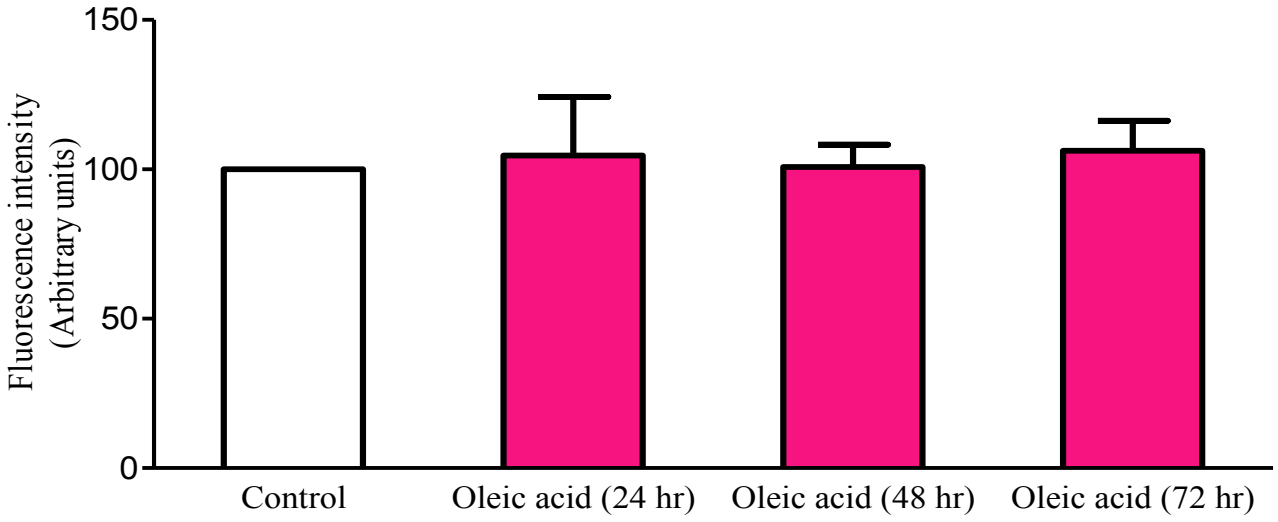

Fig 3.3 Evaluating the effects of oleic acid treatment on the degree of oxidative stress (immunofluorescence microscopy)

H9c2 cardiomyoblasts were treated with 0.25 mM oleic acid for 24 hr, 48 hr and 72 hr, respectively. Cells were analysed using immunofluorescence imaging to measure the degree of oxidative stress as described earlier (refer to section 2.4.2 of the Materials and Methods section of this thesis). – (n=3).

To assess the role of the HBP, we included DON in our experiment protocol. HBP inhibition decreased oxidative stress at the 24 and 48 hour time points (Figures 3.4 and 3.5). At the 24 hour time point DON treatment decreased oxidative stress by .57.4 ± 20.1% in comparison to DON + oleic acid (n=3, $p<0.05$). At 48 hours DON treatment decreased oxidative stress by 65.9 ± 2.9% in comparison to the control, and DON + oleic acid treatment decreased oxidative stress by 73.5 ± 5.9% in comparison to the control (n=3, $p<0.005$).

I.

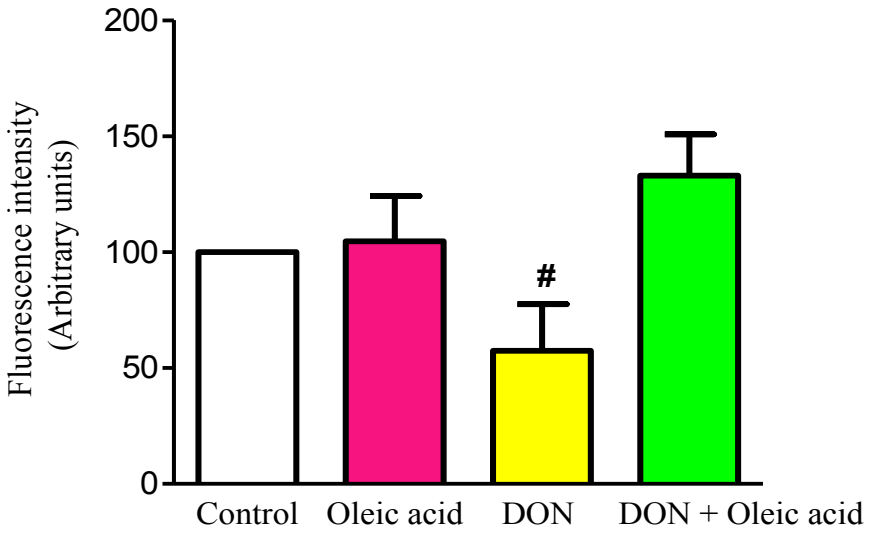

II.

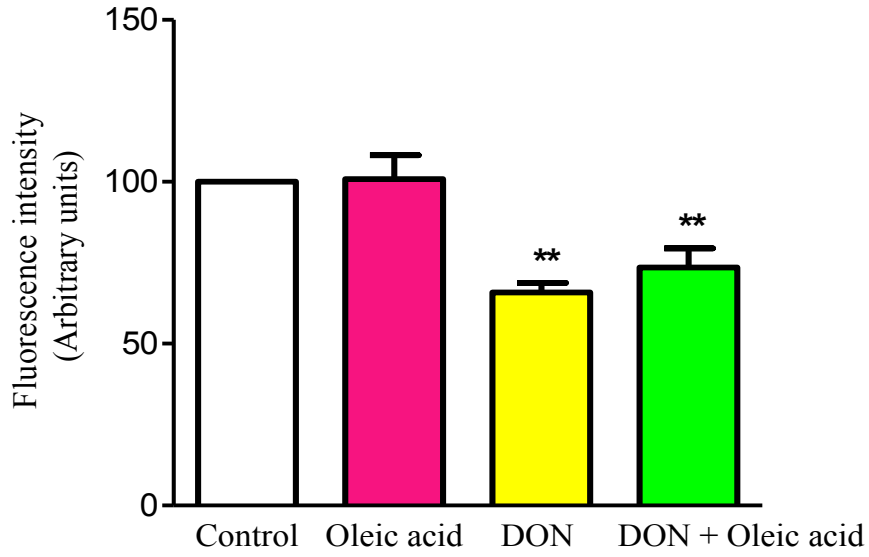

III.

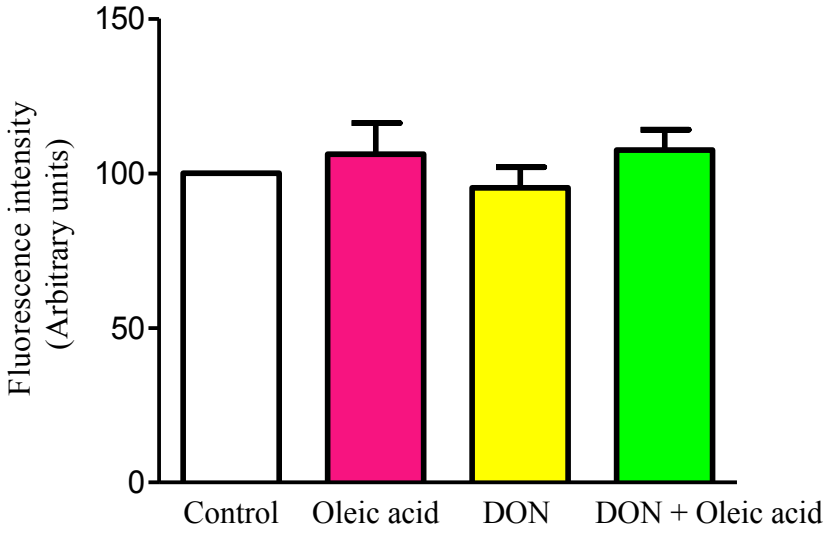

Fig 3.4 The effect of oleic acid treatment ± HBP inhibition on oxidative stress (immunofluorescence microscopy)

H9c2 cardiomyoblasts were treated with oleic acid ± DON for 24 hr (I), 48 hr (II) and 72 hr (III), respectively. Cells were analysed using immunofluorescence imaging to measure the degree of oxidative stress as described earlier (refer to section 2.4.2 of the Materials and Methods section of this thesis). ** $p<0.005$ versus control and # $p<0.05$ versus DON + oleic acid. Values are expressed as mean ± SEM – (n=3).

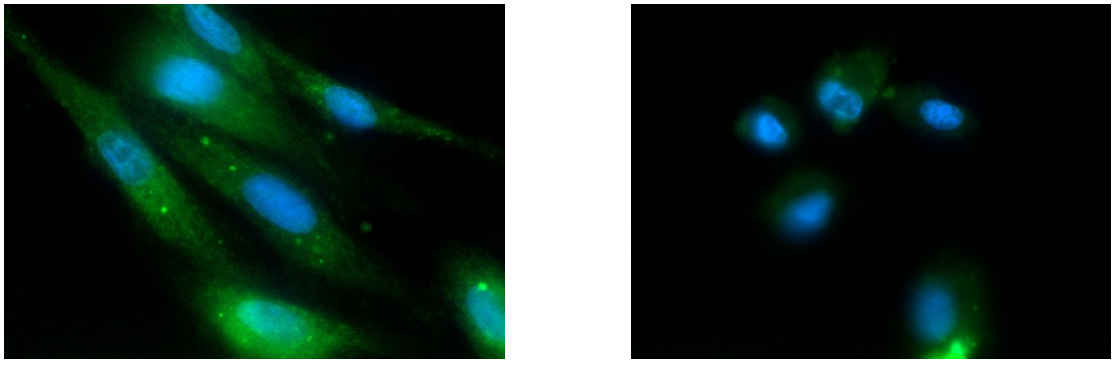

Control **Oleic acid**

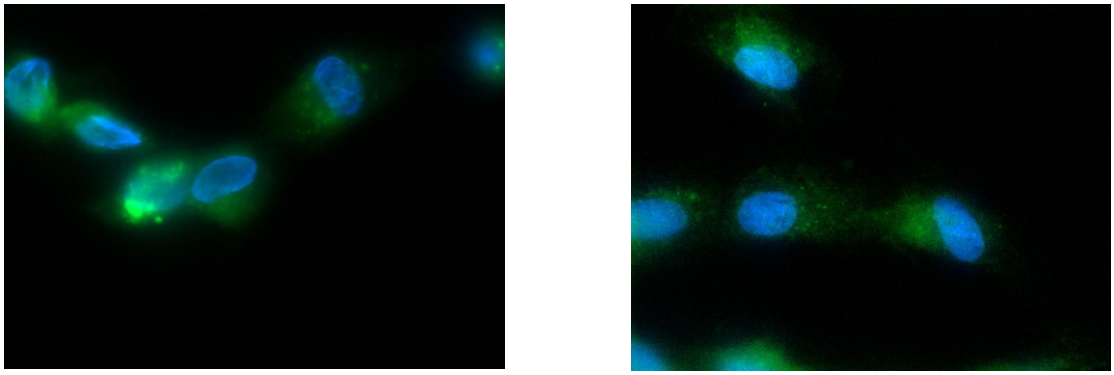

HBP inhibitor (DON) **Oleic acid + HBP inhibitor (DON)**

Fig 3.5 The effect of oleic acid treatment ± HBP inhibition on oxidative stress (immunofluorescence microscopy)

H9c2 cardiomyoblasts were treated with oleic acid ± DON for 24 hr, 48 hr and 72 hr, respectively. Cells were analysed using immunofluorescence imaging to measure the degree of oxidative stress as described earlier (refer to section 2.4.2 of the Materials and Methods section of this thesis). Cells were viewed at 100x magnification under an immunofluorescence microscope. The nucleus was stained with Hoechst (blue) stain and the rest of the cell stained green (H2DCF-DA), which is an indication of overall ROS production. Representative images were chosen from all time points to depict what is represented in the bar graphs (Fig 3.4) – (n=3).

3.3 Evaluating the level of O-GlcNAcylation: an indication of HBP flux

To evaluate HBP flux we employed a flow cyometric method to determine the degree of *O*-GlcNAcylation. The data show that *O*-GlcNAcylation increased, although this was not significant (Figure 3.6).

3.3.1 Flow cytometry

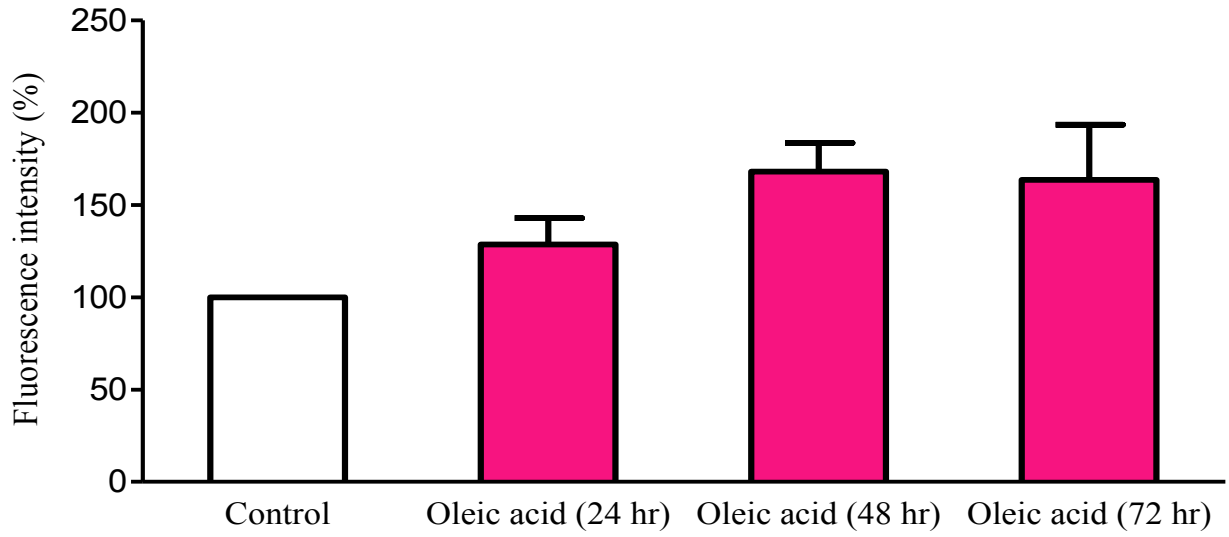

Fig 3.6 Determining the effects of oleic acid treatment on HBP activation (flow cytometry)

H9c2 cardiomyoblasts were treated with 0.25 mM oleic acid for 24 hr, 48 hr and 72 hr, respectively. Cells were analysed using flow cytometry to evaluate the level of overall *O*-GlcNAcylation as described earlier (refer to section 2.5.1 of the Materials and Methods section of this thesis). - (n=3).

Based on these findings, we decided to assess the role of the HBP at the same time intervals, but exposed to oleic and/or DON treatment to determine if it was able to diminish oleic acid-induced *O*-GlcNAcylation (Figure 3.7); supporting our data that oleic acid definitely activates the HBP in H9c2 cardiomyoblasts. This was particularly observed at 48 hours by 168.2 ± 15.5% in comparison to the control (n=3, $p<0.005$) as well as at 72 hours by 163.7 ± 29.8% in comparison to the control (n=3, $p<0.05$). However, DON treatment inhibited HBP activation at 24 hours by 88.7 ± 4.1%; 48 hours by 119.3 ± 8.0% and at 72 hours by 86.1% ± 6.3% in comparison to oleic acid (n=3, $p<0.05$). Additionally, DON + oleic acid treatment decreased levels of *O*-GlcNAcylation at 72 hours by 87.5 ± 4.8% in comparison to oleic acid (n=3, $p<0.05$).

I.

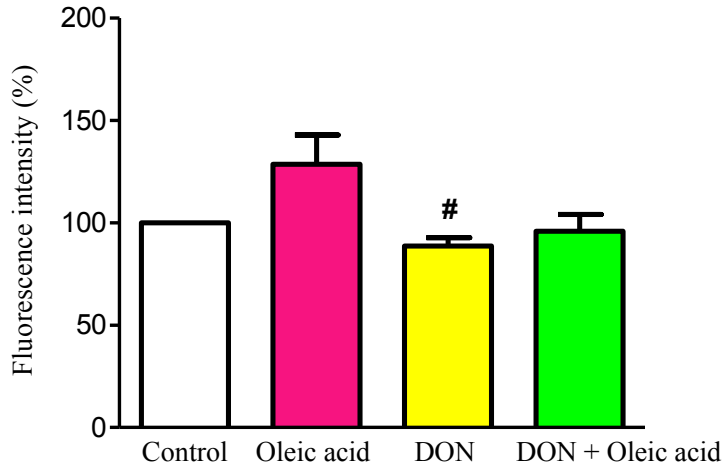

II.

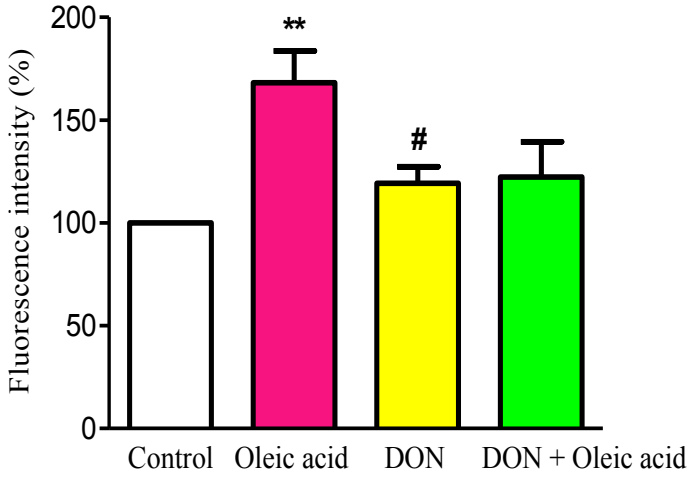

III.

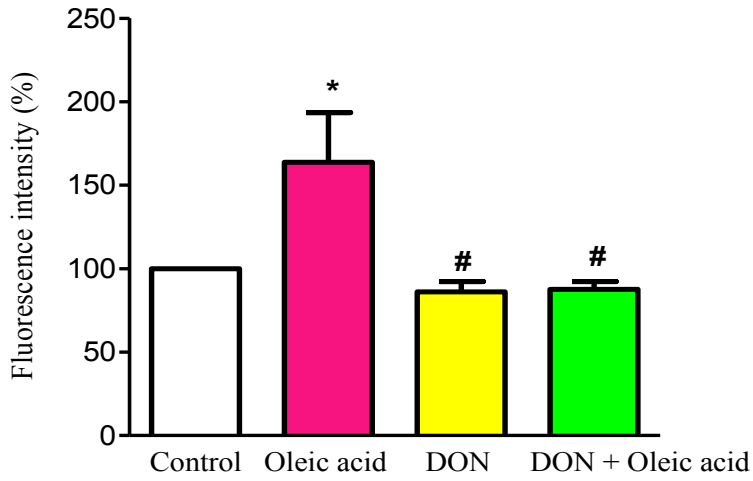

Fig 3.7 The effect of oleic acid treatment ± HBP inhibition on *O*-GlcNAcylation (flow cytometry)

H9c2 cardiomyoblasts were treated with oleic acid ± DON for 24 hr (I), 48 hr (II) and 72 hr (III), respectively. Cells were analysed using flow cytometry to evaluate the level of overall *O*-GlcNAcylation as described earlier (refer to section 2.5.1 of the Materials and Methods section of this thesis). * $p<0.05$ versus control, ** $p<0.005$ versus control, # $p<0.05$ versus oleic acid. Values are expressed as mean ± SEM - (n=3).

3.3.2 Immunofluorescence microscopy

Immunofluorescence imaging evaluated overall O-GlcNAcylation but, we found no significant changes with oleic acid treatment using this method (Figure 3.8).

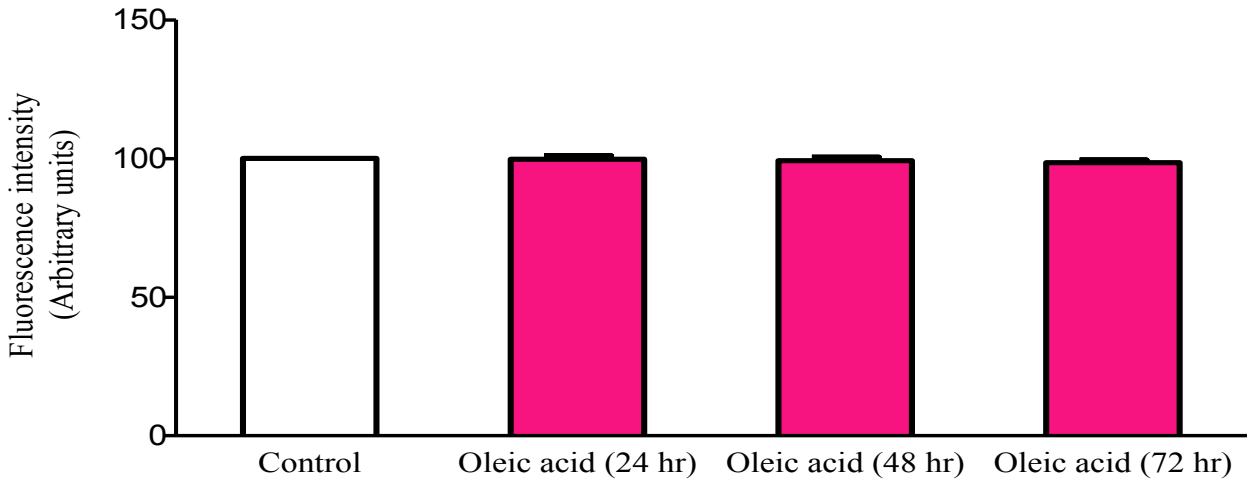

Fig.3.8 The effect of oleic acid on HBP flux (immunofluorescence microscopy)

H9c2 cardiomyoblasts were treated with 0.25 mM oleic acid 24 hr, 48 hr and 72 hr, respectively. Cells were viewed under the immunofluorescence microscopy to evaluate overall *O*-GlcNAcylation, as described in the Materials and Methods section of this thesis (refer to section 2.5.2) - (n=3).

The same trend was found after DON treatment with no significant changes (Figures 3.9 and 3.10).

I.

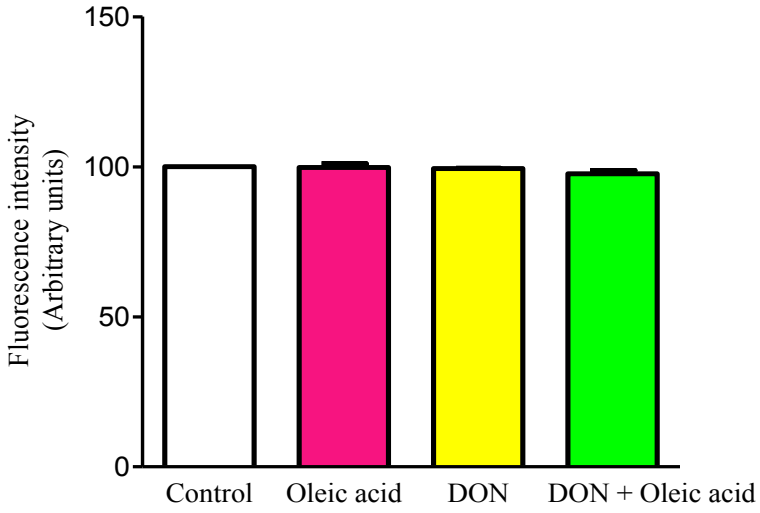

II.

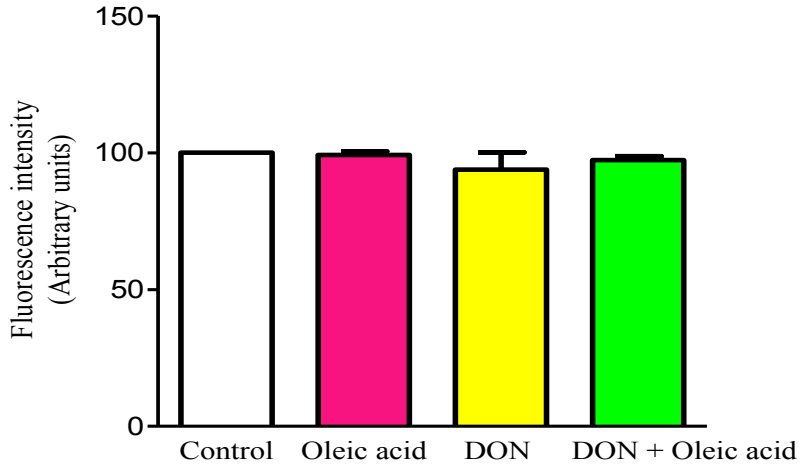

III.

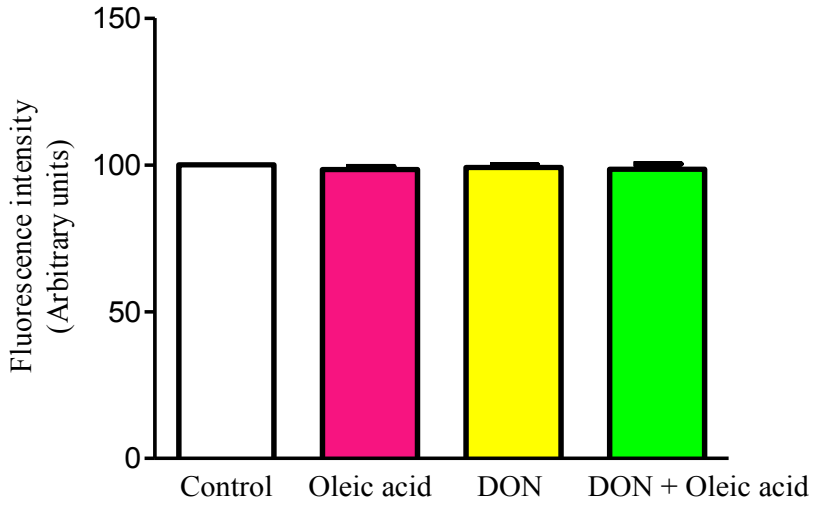

Fig 3.9 The effect of oleic acid treatment ± HBP inhibitor on HBP flux (immunofluorescence microscopy)

H9c2 cardiomyoblasts were treated with oleic acid ± DON for 24 hr (I), 48 hr (II) and 72 hr (III), respectively. The cells were viewed using immunofluorescence imaging to evaluate overall *O*-GlcNAcylation, as described in the Materials and Methods section of this thesis (refer to section 2.5.1) - (n=3).

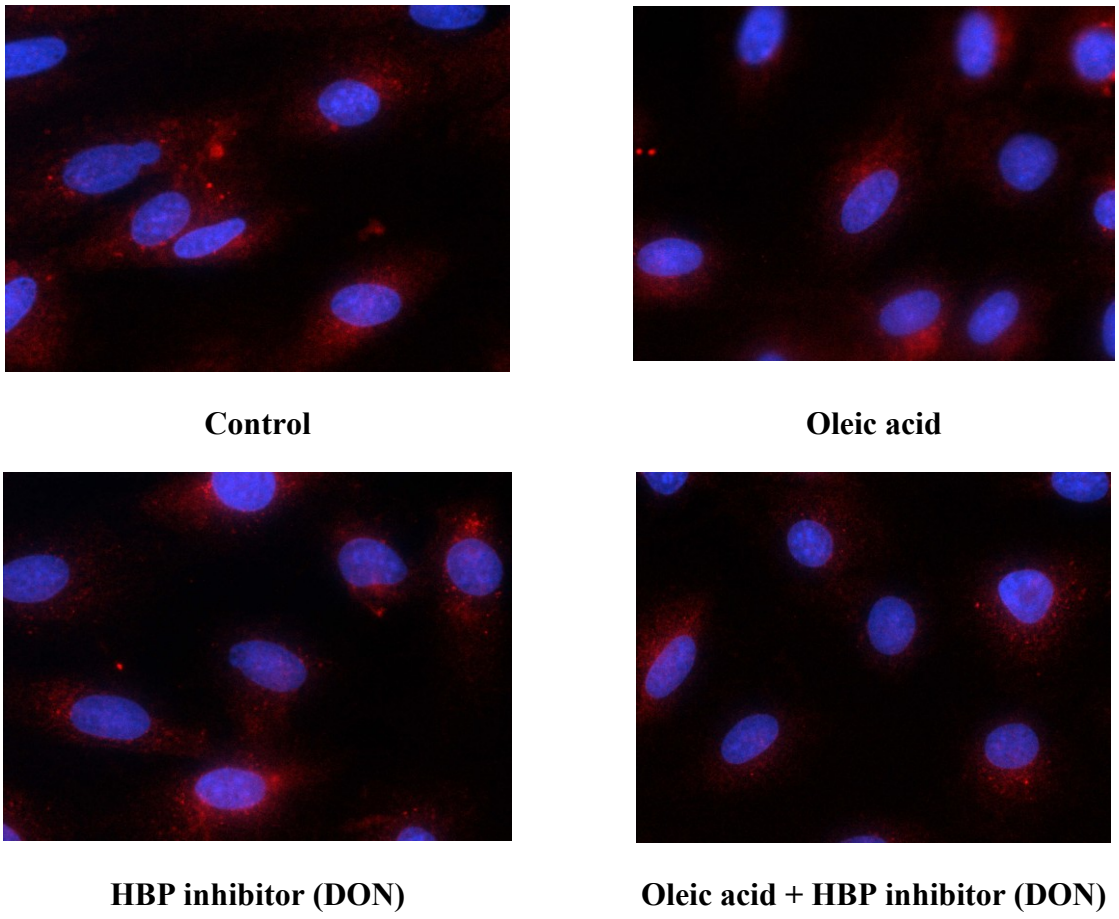

Fig 3.10 The effect of oleic acid treatment ± HBP inhibitor on HBP flux (immunofluorescence microscopy)

H9c2 cardiomyoblasts were treated with oleic acid ± DON for 24 hr, 48 hr and 72 hr, respectively. The cells were viewed using immunofluorescence imaging to evaluate overall *O*-GlcNAcylation, as described in the Materials and Methods section of this thesis (refer to section 2.5.1). Cells were viewed at 100x magnification under an immunofluorescence microscope. The nucleus was stained with Hoechst (blue) stain and the rest of the cell stained red (Texas Red), which is an indication of overall *O*-GlcNAcylation. Representative images were chosen from all time points to depict what is represented in the bar graphs (Fig. 3.9) - (n=3).

3.4 Assessment of apoptosis

To evaluate the effects of oleic acid on cell death, i.e. apoptosis and necrosis it was found that oleic acid treatment markedly reduced apoptotic cell death as assessed by flow cytomery (Figure 3.11). Apoptosis was attenuated at 24 hours by 0.7 ± 0.2% ; 48 hours by 1.1 ± 0.3% and at 72 hours by 1.0 ± 0.2% in comparison to the control [4.7 ± 1.3% (n=3, $p<0.005$)].

3.4.1 Flow cytometry: Propidium iodide & Annexin V staining

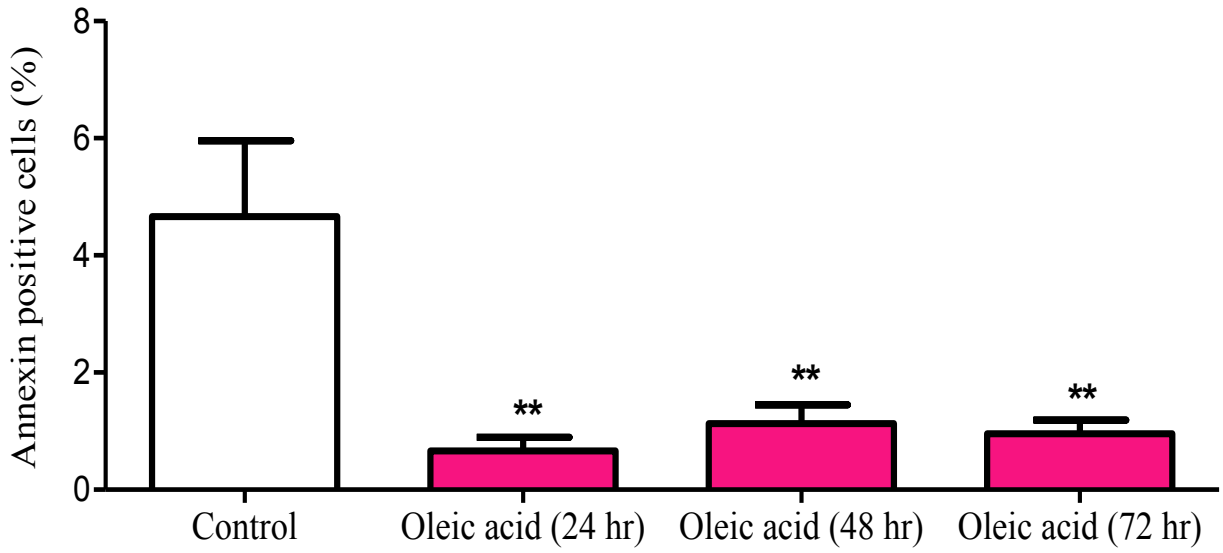

Fig 3.11 Evaluating the anti-apoptotic effects of oleic acid (flow cytometry)

H9c2 cardiomyoblasts were treated with 0.25 mM oleic acid for 24 hr, 48 hr and 72 hr, respectively. The cells were analysed using flow cytometry to assess apoptosis as described in the Materials and Methods section of this thesis (refer to section 2.6.1). ** $p<0.005$ versus control. Values are expressed as mean ± SEM - (n=3).

We subsequently tested the role of the HBP within this context. Oleic acid treatment resulted in an anti-apoptotic phenotype as before (Figure 3.12). This concept was observed at 24 hours where oleic acid decreased apoptosis by 1.2 ± 0.6% in comparison to the control [4.7 ± 1.3% (n=3, $p<0.005$)], as well as at 72 hours by 1.0 ± 0.2% in comparison to the control [4.7 ± 1.3% (n=3, $p<0.05$)]. However, DON had an even greater anti-apoptotic effect. DON treatment also further decreased the anti-apoptotic effects of oleic acid (Figure 3.12). DON decreased apoptosis at 24 hours by 0.7 ± 0.3% as well as at 72 hours by 0.9 ± 0.2% in comparison to the control [4.7 ± 1.3% (n=3, $p<0.05$)]. Additionally, an additive effect was observed when the cardiomyoblasts were treated with DON and oleic acid. The combined treatment decreased apoptosis at 24 hours by 0.6 ± 0.1% in comparison to the control [4.7 ± 1.3% (n=3, $p<0.05$)]., and at 72 hours by 0.6 ± 0.2% in comparison to the control [4.7 ± 1.3% (n=3, $p<0.005$)]. At the 48 hour time point there was also a downward trend observed with regard to apoptosis, although this was not significant.

I.

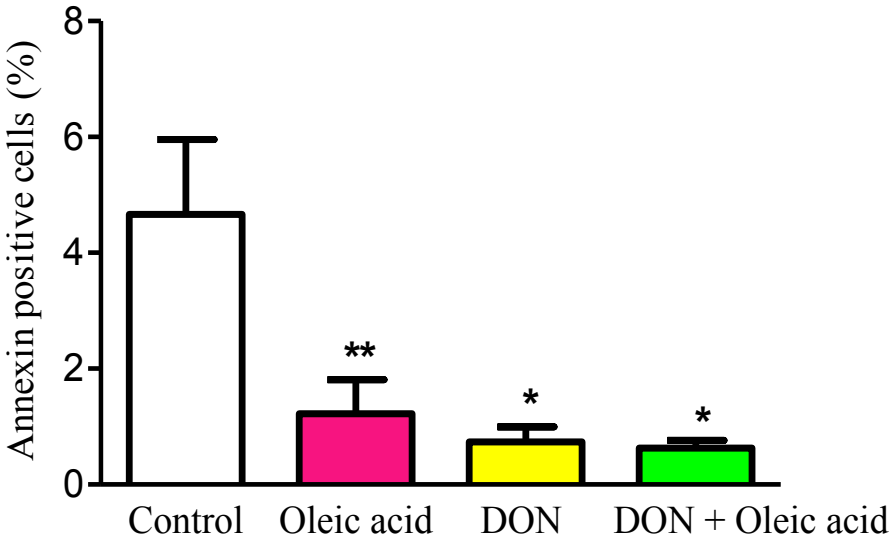

II.

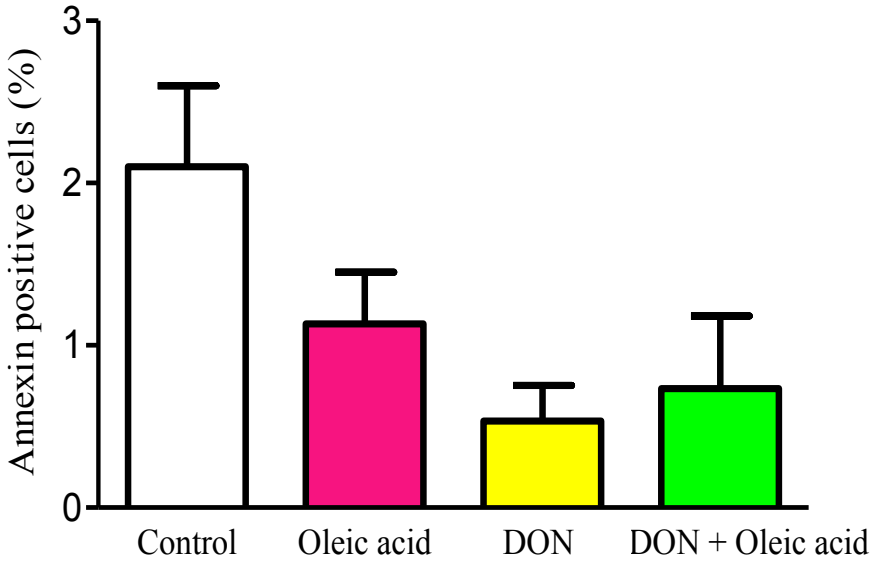

III.

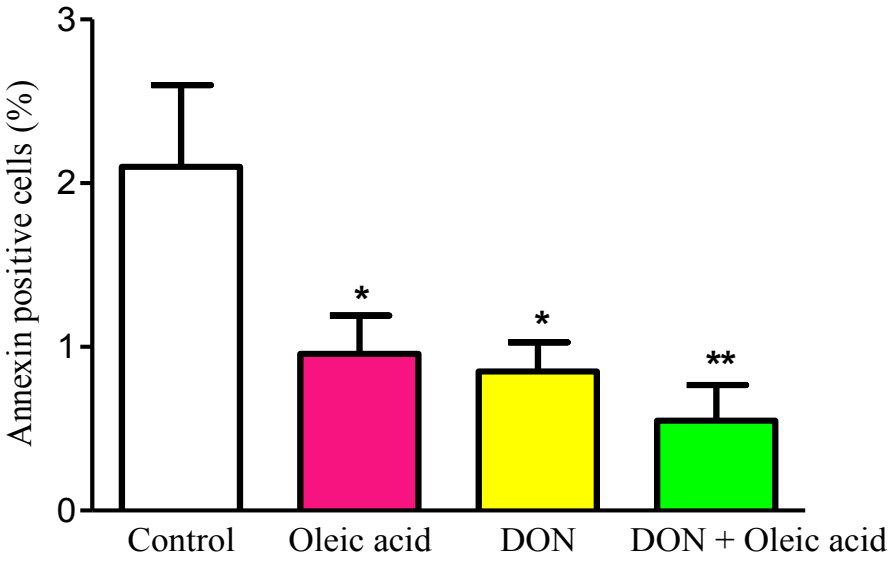

Fig 3.12 Evaluating the anti-apoptotic effects of HBP inhibition (flow cytometry)

H9c2 cardiomyoblasts were treated with oleic acid ± DON for 24 hr (I), 48 hr (II) and 72 hr (III), respectively. Cells were analysed using flow cytometry to assess apoptosis as described in the Materials and Methods section of this thesis (refer to section 2.6.1). * $p<0.05$ versus control,

** $p<0.005$ versus control. Values expressed as mean ± SEM - (n=3).

3.4.2 Immunofluorescence microscopy: Hoechst staining

To establish repeatability and validity the protocol was repeated using immunofluorescence microscopy to view the apoptotic nuclei. We found no significant changes when using this technique (Figure 3.13).

I.

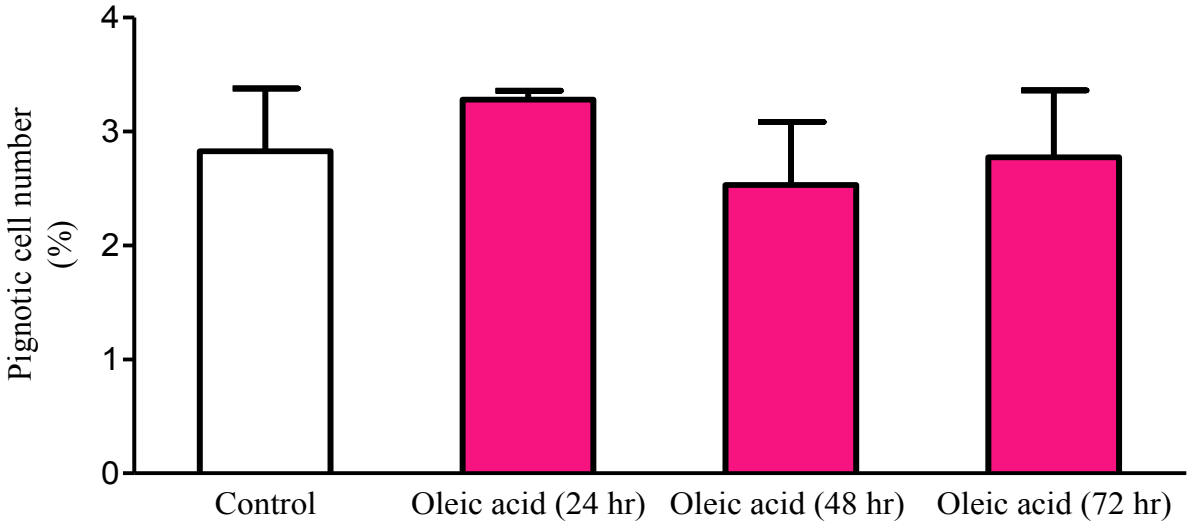

Fig 3.13 The anti-apoptotic effects of oleic acid (immunofluorescence microscopy)

H9c2 cardiomyoblasts were treated with 0.25 mM oleic acid for 24 hr, 48 hr and 72 hr, respectively. The cells were analysed using immunofluorescence imaging to assess apoptosis as described in the Materials and Methods section of this thesis (refer to section 2.6.2). - (n=3).

We next evaluated the role of the HBP when the cells were exposed to oleic acid and/or DON. The data shows, a downward trend in apoptosis mainly at the 72 hour time point, although this was not a significant change (Figures 3.14 and 3.15).

I.

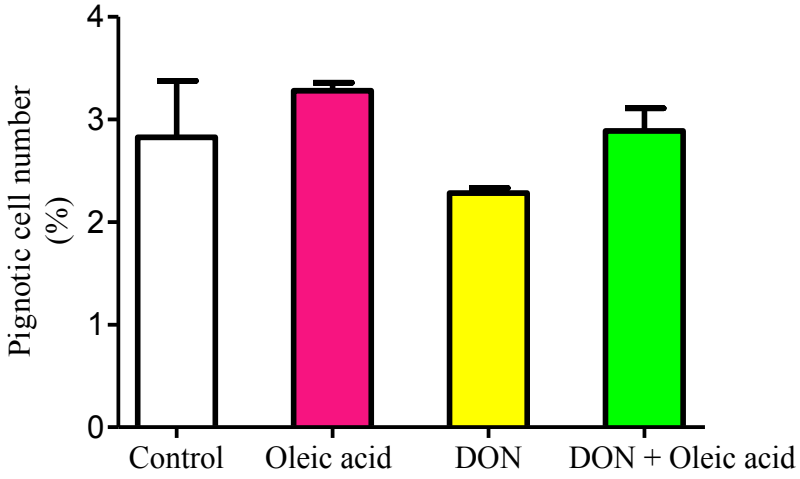

II.

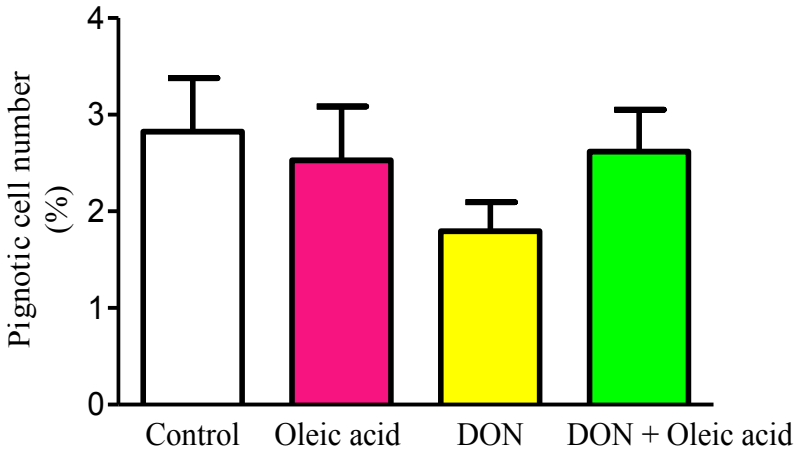

III.

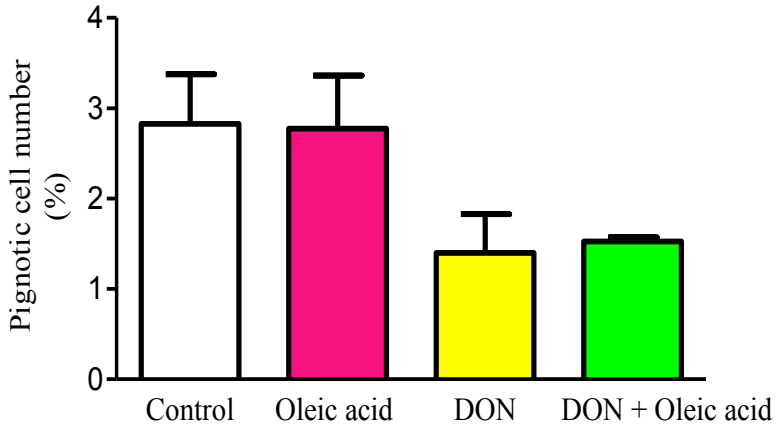

Fig 3.14 The anti-apoptotic effects of HBP inhibition (immunofluorescence microscopy)

H9c2 cardiomyoblasts were treated with oleic acid ± DON for 24 hr (I), 48 hr (II) and 72 hr (III), respectively. Cells were viewed using immunofluorescence microscopy to assess apoptosis as described in the Materials and Methods section of this thesis (refer to section 2.6.2) - (n=3).

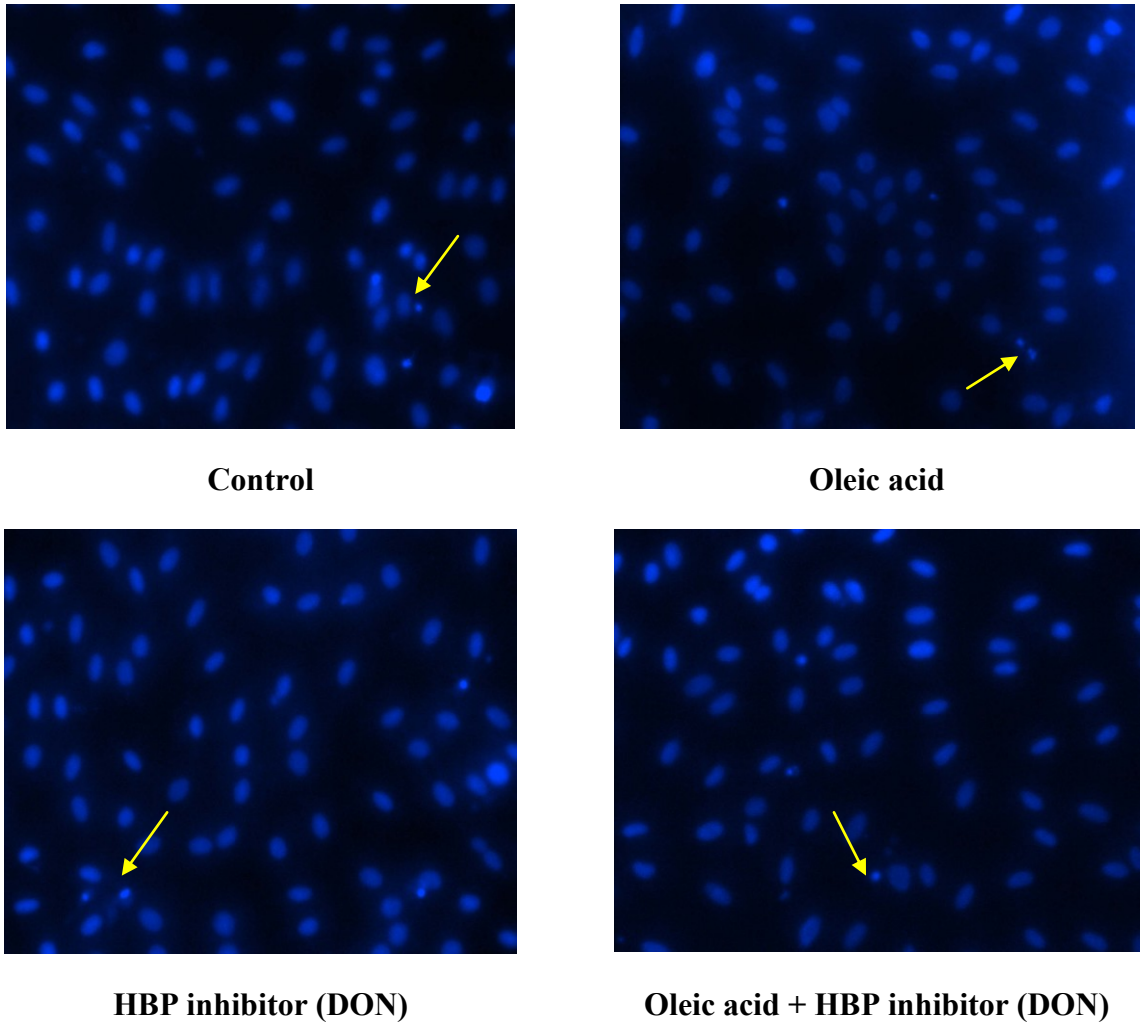

Fig. 3.15 The anti-apoptotic effects of HBP inhibition (immunofluorescence microscopy)

H9c2 cardiomyoblasts were treated with oleic acid ± DON for 24 hr, 48 hr and 72 hr, respectively. Cells were viewed using immunofluorescence microscopy to assess apoptosis as described in the Materials and Methods section of this thesis (refer to section 2.6.2). Cells were viewed at 40x magnification under an immunofluorescence microscope. The nucleus was stained with Hoechst (blue) stain to identify apoptotic nuclei. Yellow arrows indicate apoptotic nuclei that are either condensed or fragmented of which there were only a few apoptotic cells, hence, there being no significant differences between treatment groups as depicted in the bar graphs (Fig. 3.14). Representative images were chosen from all time points to depict what is represented in the bar graphs - (n=3).

3.5 Caspase-Glo 3 assay

To confirm our apoptosis data obtained by flow cytometry and immunofluorescence microscope imaging, we also assessed apoptosis by using a luminescence-based caspase assay. Our data confirmed that oleic acid treatment results in anti-apoptotic effects, although the changes were not significant (Figure 3.16).

III.

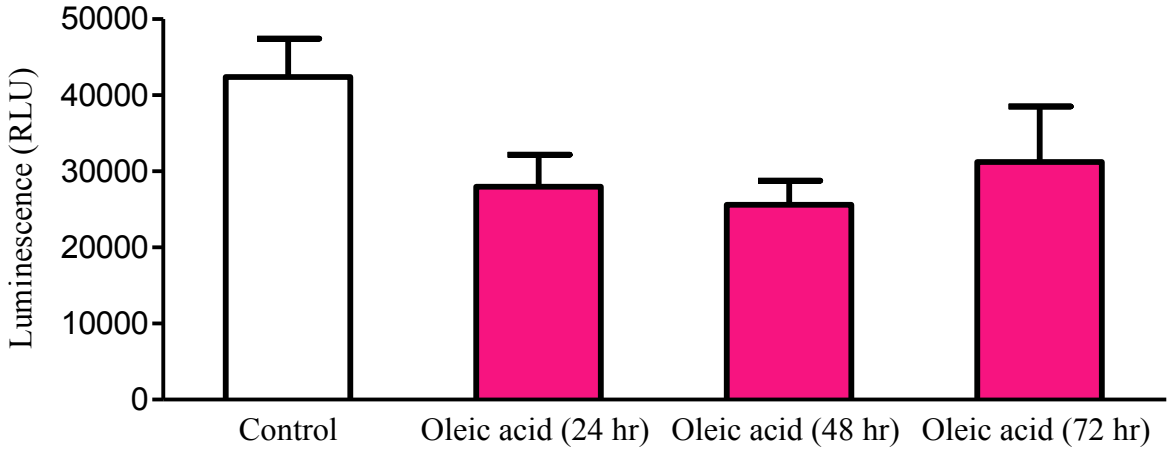

Fig 3.16 Evaluating the anti-apoptotic effects oleic acid (caspase assay)

H9c2 cardiomyoblasts were treated with 0.25 mM oleic acid for 24 hr, 48 hr and 72 hr, respectively. Cells were analysed using luminescence to assess apoptosis as described in the Materials and Methods section of this thesis (refer to section 2.6.3). - (n=3). RLU: Relative Luciferase Units.

To evaluate the role of the HBP, we treated cells with DON and found (as before) that it decreased apoptosis (Figure 3.17). At 24 hours there was a downward trend in apoptosis, although this was not significant decreases. At 48 hours however, oleic acid attenuated apoptosis by 25614 ± 3171% in comparison to the control [42379 ± 5064% (n=3, $p<0.05$)]. However, DON inhibited the effects of the HBP, and like oleic acid, also showed anti-apoptotic effects at 48 hours where apoptosis was decreased by 17391 ± 1938% in comparison to the control [42379 ± 5064% (n=3, $p<0.005$)], as well as at 72 hours where DON decreased apoptosis by 13116 ± 189.2% in comparison to the control [42379 ± 5064% (n=3, $p<0.005$)], and by 13116 ± 189.2% in comparison to oleic acid [31235 ± 7300% (n=3, $p<0.05$)]. However, co-treatment with DON and oleic acid did not further decrease the anti-apoptotic effects of sole oleic acid treatment, although it did decrease apoptosis at 48 hours by 29484 ± 3818% in comparison to the control [42379 ± 5064% (n=3, $p<0.05$)], and at 72 hours by 12838 ± 1356% in comparison to the control [42379 ± 5064% (n=3, $p<0.005$)], and by 12838 ± 1356% in comparison to oleic acid [31235 ± 7300% (n=3, $p<0.05$)],

I.

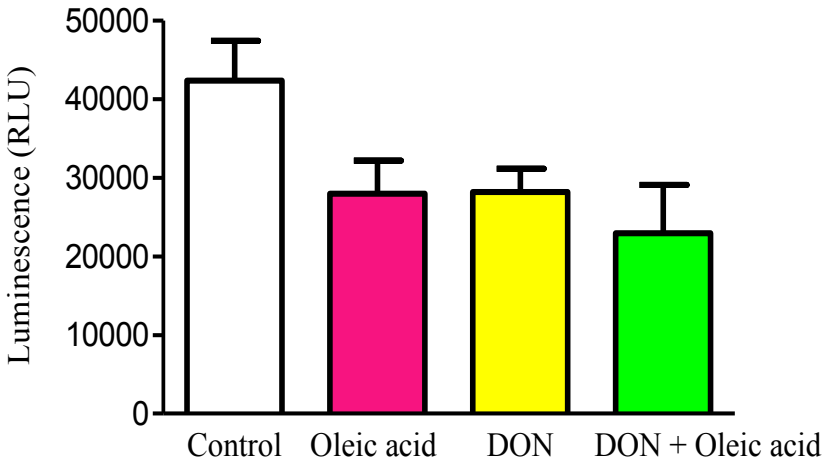

II.

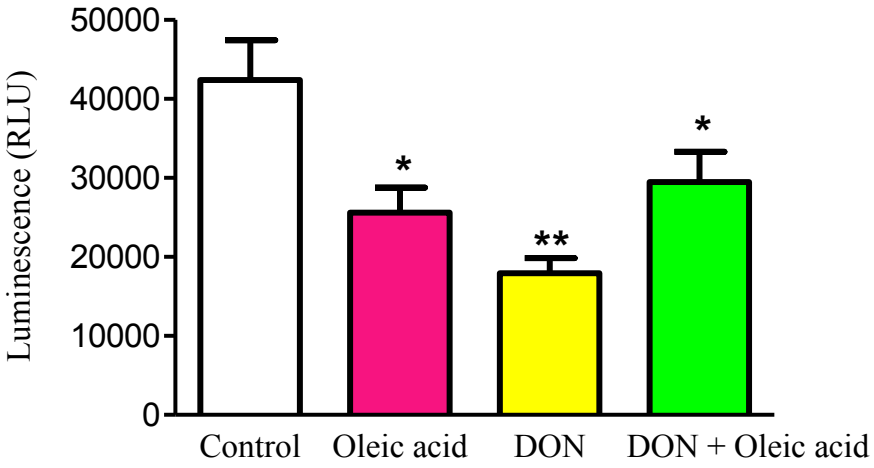

III.

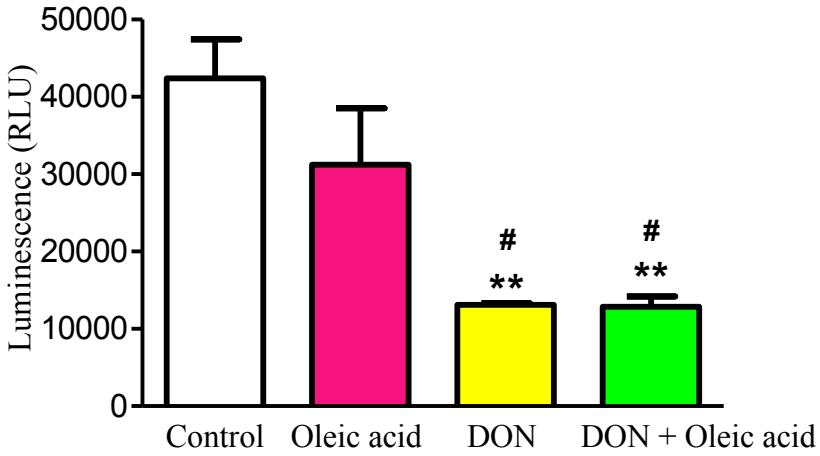

Fig 3.17 Evaluating the anti-apoptotic effects of the HBP inhibitor (Caspase assay).

H9c2 cardiomyoblasts were treated with oleic acid ± DON for 24 hr (I), 48 hr (II) and 72 hr (III), respectively. The cells were analysed using luminescence to assess apoptosis as described in the Materials and Methods section of this thesis (refer to section 2.6.3). * $p<0.05$ versus control, ** $p<0.005$ versus control, # $p<0.05$ versus oleic acid, Values are expressed as mean ± SEM - (n=3). RLU: Relative Luciferase Units.

3.6 Assessment of necrosis

We also evaluated the effects of oleic acid treatment on necrosis (by flow cytometry). Our data show that oleic acid treatment decreased necrotic cell death after 48 hours of treatment (Figure 3.18). Oleic acid decreased necrosis at 48 hours by 1.0 ± 0.2% in comparison to the control [1.6 ± 0.2% (n=3, $p<0.05$)], and by 1.0 ± 0.2% in comparison to both 24 hours [1.8 ± 0.2% (n=3, $p<0.05$)] and 72 hours [2.0 ± 0.1% (n=3, $p<0.05$)].

3.6.1 Flow cytometry: Propidium iodide & Annexin V staining

I.

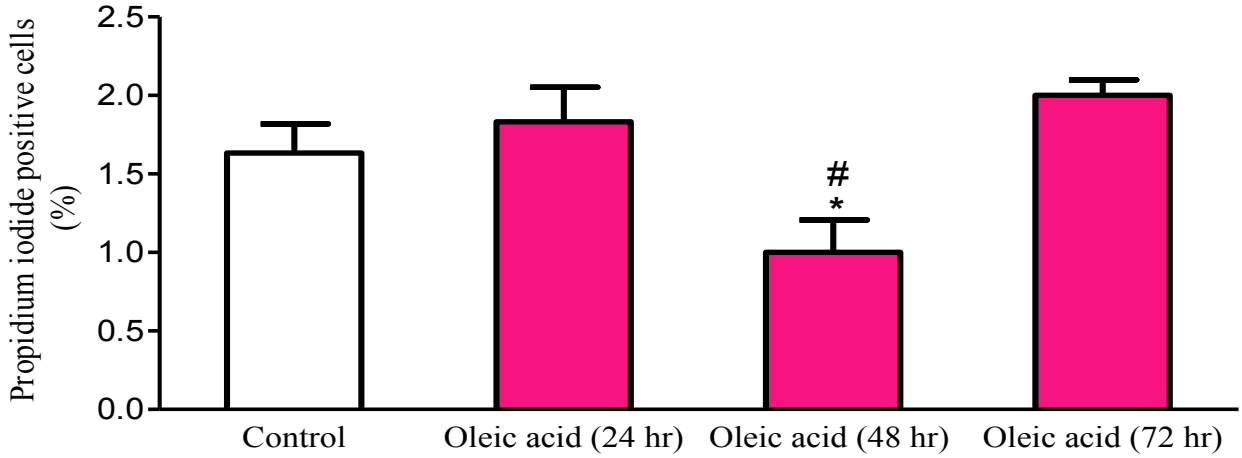

Fig 3.18 Evaluating the anti-necrotic effects of oleic acid (flow cytometry)

H9c2 cardiomyoblasts were treated with 0.25 mM oleic acid for 24 hr, 48 hr and 72 hr, respectively. The cells were analysed using flow cytometry to assess necrosis as described in the Materials and Methods section of this thesis (refer to section 2.6.1).* $p<0.05$ versus control, # $p<0.05$ versus oleic acid 24 hr and 72 hr. Values are expressed as mean ± SEM - (n=3).

Sole DON treatment also resulted in robust anti-necrotic effects (Figure 3.19), whereby DON decreased necrosis at 24 hours by 1.1 ± 0.2% in comparison to oleic acid [1.8 ± 0.2% (n=3, $p<0.05$)], and at 72 hours by 1.0 ± 0.2% in comparison to oleic acid [2.0 ± 0.1% (n=3, $p<0.05$)]. When the cardiomyoblasts were treated with DON + oleic acid, a decrease in necrosis was noted at 24 hours by 1.0 ± 0.2% in comparison to oleic acid [1.8 ± 0.2% (n=3, $p<0.05$)], although this was not an additive effect in comparison to the sole treatment of oleic acid and DON. Additionally, a downward trend in necrosis was noted at 48 hours, but it was not a significant trend.

I.

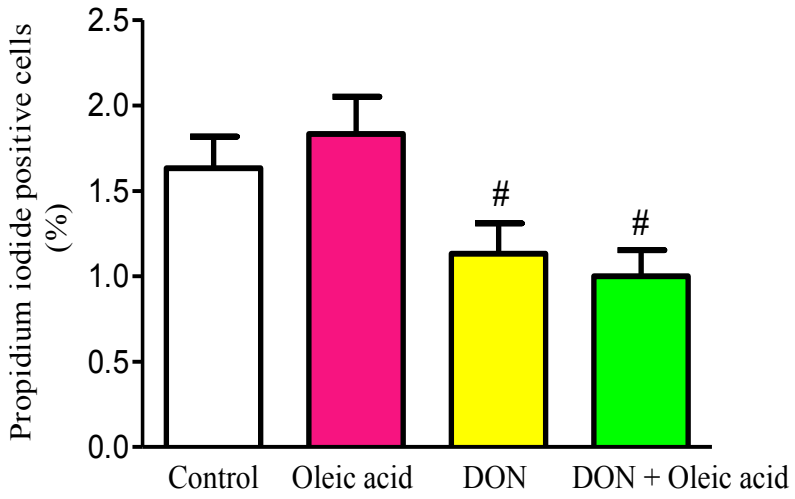

II.

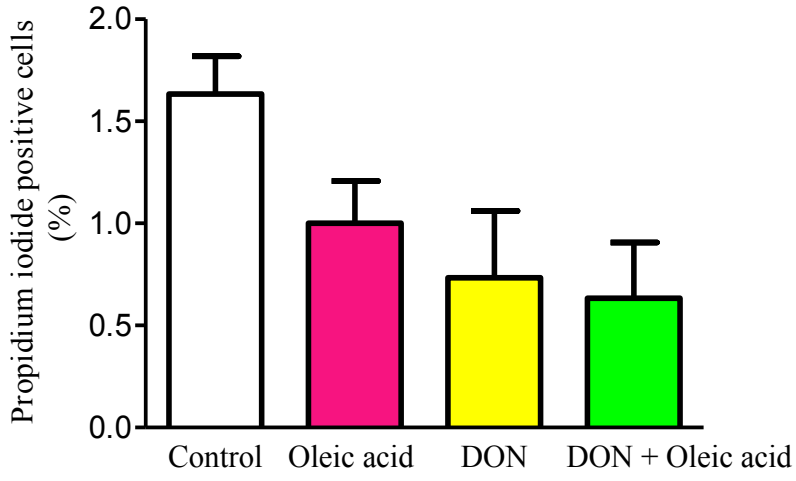

III.

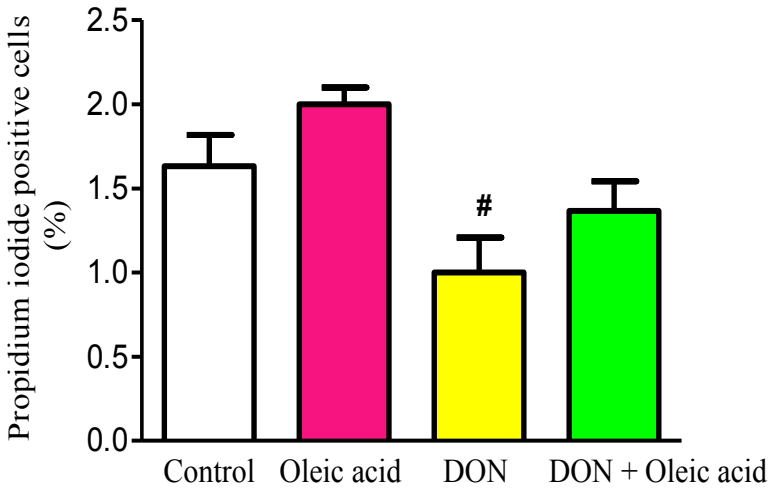

Fig 3.19 Evaluating the anti-necrotic effects of HBP inhibition (flow cytometry)

H9c2 cardiomyoblasts were treated with oleic acid ± DON for 24 hr (I), 48 hr (II) and 72 hr (III), respectively. The cells were analysed using flow cytometry to assess necrosis as described in the Materials and Methods section of this thesis (refer to section 2.6.1). # $p<0.05$ versus oleic acid. Values are expressed as mean ± SEM - (n=3).

Chapter 4: Discussion

4.1 Introduction

Obesity and type 2 diabetes are two common pre-disposing factors for cardiovascular disease; it has been estimated that the prevalence of obesity will increase to ~1.35 billion by 2030 [6]. There are, however, a number of factors that play a role in individuals becoming obese and unhealthy, but for the present study, we focused on increased fatty acid supply and its impact on the HBP and cell death.

Here we ventured in the opposite direction and investigated whether oleic acid acts as a novel cardioprotective agent. We further examined whether this effect occurred via the HBP. The key findings of this study are: *1) Oleic acid blunts oxidative stress and cell death (apoptosis and necrosis) in H9c2 cells; 2) Oleic acid activates the HBP; and 3) There is no cross-talk between HBP activation and oleic acid-mediated reduction of oxidative stress and cell death*.

4.2 Oleic acid blunts oxidative stress and cell death in H9c2 cardiomyoblasts

We initially tested whether oleic acid acts as an anti-oxidant. The flow cytometry data show that oxidative stress was significantly decreased after 48 hours of treatment. The data therefore indicate a peak response at the 48 hour time point. We propose that this may be due to the time necessary to initiate downstream effects (e.g. composition of biological membranes and activation of transcriptional mechanisms) that are later discussed. We largely confirmed flow cytometric data by employing immunofluorescent microscopy, where slight changes was observed between treatments.

How does oleic acid reduce oxidative stress? We have been unable to pursue this question in the present study, but wish to make several proposals (based on the literature) of how this may transpire.

In the first instance, it is likely that this may occur by protecting biological membranes, e.g. the sarcolemma and mitochondrial membrane. The degree of saturation of membranes increases the sensitivity to lipid peroxidation, i.e. increased number of double bonds per molecule and a greater number of unstable electrons. De Vries *et al*. (1997) [2] found that in response to oleic acid exposure, neonatal cardiomyocytes increased the percentage of mono-unsaturated fatty acids in the phospholipid pool by approximately 3-fold [16]. Thus, the supply of a monounsaturated fatty acid like oleic acid may increase the degree of unsaturation and thereby attenuate intracellular oxidative stress. In agreement, others [12] found that consumption of virgin olive oil lowered peroxidation in liver mitochondria and microsomes. Here the concept proposed is that the type of dietary fat affects biological membrane function, e.g. mitochondrial membranes and their susceptibility to oxidative stress [5, 10, 12-13].

Another possible mechanism that may explain our findings is the proposal that oleic acid may increase intracellular anti-oxidant capacity. Rats fed palm olein oil (rich in oleic acid; 42.7 – 43.9%) [3, 8-9] displayed elevated myocardial catalase, superoxide dismutase and glutathione peroxidase activities [8]. This was associated with increased protection of hearts in response to ischemia-reperfusion damage. Thus, we propose that oleic acid may exert its anti-oxidant effects by enhancing biological membrane function(s) and/or by increasing intracellular anti-oxidant capacity. These interesting possibilities require further investigations in our experimental system.

Testing whether oleic acid administration was able to inhibit cell death in H9c2 cardiomyoblasts we found that oleic acid decreased apoptosis at all three time points (flow cytometry). When DON was administered to these cells, apoptosis was also decreased, and with a combination treatment of DON + oleic acid, and additive effect was observed at 24 and 72 hours. These data was also confirmed by a caspase activity analysis and immunofluorescent microscopy. In the caspase assay apoptosis was significantly decreased at 48 hours, but it was not significantly decreased at 24 hours. At 72 hours the DON and DON + oleic acid treatment decreased apoptosis. For immunofluorescence microscopy, a downward trend in apoptosis was observed, although this was not significant. Moreover, our data show that oleic acid treatment also inhibited necrosis, particularly at 48 hours.

It is unclear whether oleic acid directly affects apoptosis and necrosis pathways, or whether these effects occur secondarily to the reduction in oxidative stress. Since oxidative stress plays a key role in triggering both apoptosis and necrosis pathways [14, 15] it is likely that this scenario may hold in this experimental model. However, further studies are required to confirm this, e.g. we are planning to include an anti-oxidant in our experimental system and then test its effect on apoptosis and necrosis, respectively.

It is also possible that there may be direct effects (i.e. not related to decreased oxidative stress) mediated by oleic acid found that upregulated PI3K is upregulated an anti-apoptotic factor, in cultured breast cancer cells [4]. PI3K activation enhances cell survival and blunts apoptosis via its downstream target, Akt /PKB [3, 11]. Moreover, elevated monounsaturated fatty acids in the phospholipid pool may increase membrane fluidity and thereby decrease

apoptosis [2, 16]. Here the idea is put forward that alterations in the composition of phospholipid membranes may act as a trigger for apoptosis [17], e.g. increased saturated fatty acids may impair membrane fluidity and increase apoptosis [16].

A further possibility is that oleic acid may have transcriptional effects in the nucleus. Previous research has shown that oleic acid upregulated Bcl-2 levels in pancreatic β-cells and thereby protected against saturated fat-mediated apoptosis. Increased Bcl-2 availability will be expected to inhibit cytochrome-c release from the mitochondrion and thereby limit the apoptotic cascade [7]. Oleic acid may facilitate triglyceride accumulation (inert) in non-adipocytes and thereby decrease lipotoxic effects of 'active' lipid derivatives, e.g. ceramide-mediated apoptosis [2]. These possibilities require further investigation in our protocol.

4.3 Oleic acid activates the HBP

A novel finding, as far as we are aware, is that oleic acid increased the overall *O*-GlcNAcylation (by flow cytometric analysis) at 48 and 72 hours, suggesting increased HBP flux. However, we were unable to confirm these findings by immunofluorescent microscopy. Furthermore, we feel confident about our flow cytometric data since we typically screened 5,000 cells while the selection of representative cells (immunofluorescent microscopy) was difficult at times.

How does oleic acid activate the HBP? We propose that this may occur via the Randle effect in which higher fatty acid oxidation rates lead to PDH and PFK inhibition (refer to Fig 1.2 in the Introduction).

Subsequently, there may be an accumulation of upstream metabolites that could enter the HBP and result in increased *O*-GlcNAcylation as found in our research. Acetyl-CoA

produced from increased fatty acid oxidation can also enter the HBP, i.e. required for the correction of glucosamine-6-phosphate to GlcNAc-6-phosphate.

4.4 No cross-talk between HBP activation and oleic acid-mediated reduction of oxidative stress and cell death

The data show that oleic acid treatment triggers distinct cardioprotective pathways and that this does not occur solely via HBP activation. We also found that HBP inhibition (using DON) resulted in decreased oxidative stress and attenuated cell death (apoptosis and necrosis). However, when oleic acid and HBP inhibition were combined, no additive effects were observed in terms of downstream effects, i.e. degree of oxidative stress and cell death. Figure 4.1 shows several possible scenarios that may occur. Since we found oleic acid increases the HBP, there are two possible outcomes, i.e. pathway #1 (increased ROS, increased cell death) versus pathway #2 (decreased ROS, decreased cell death).

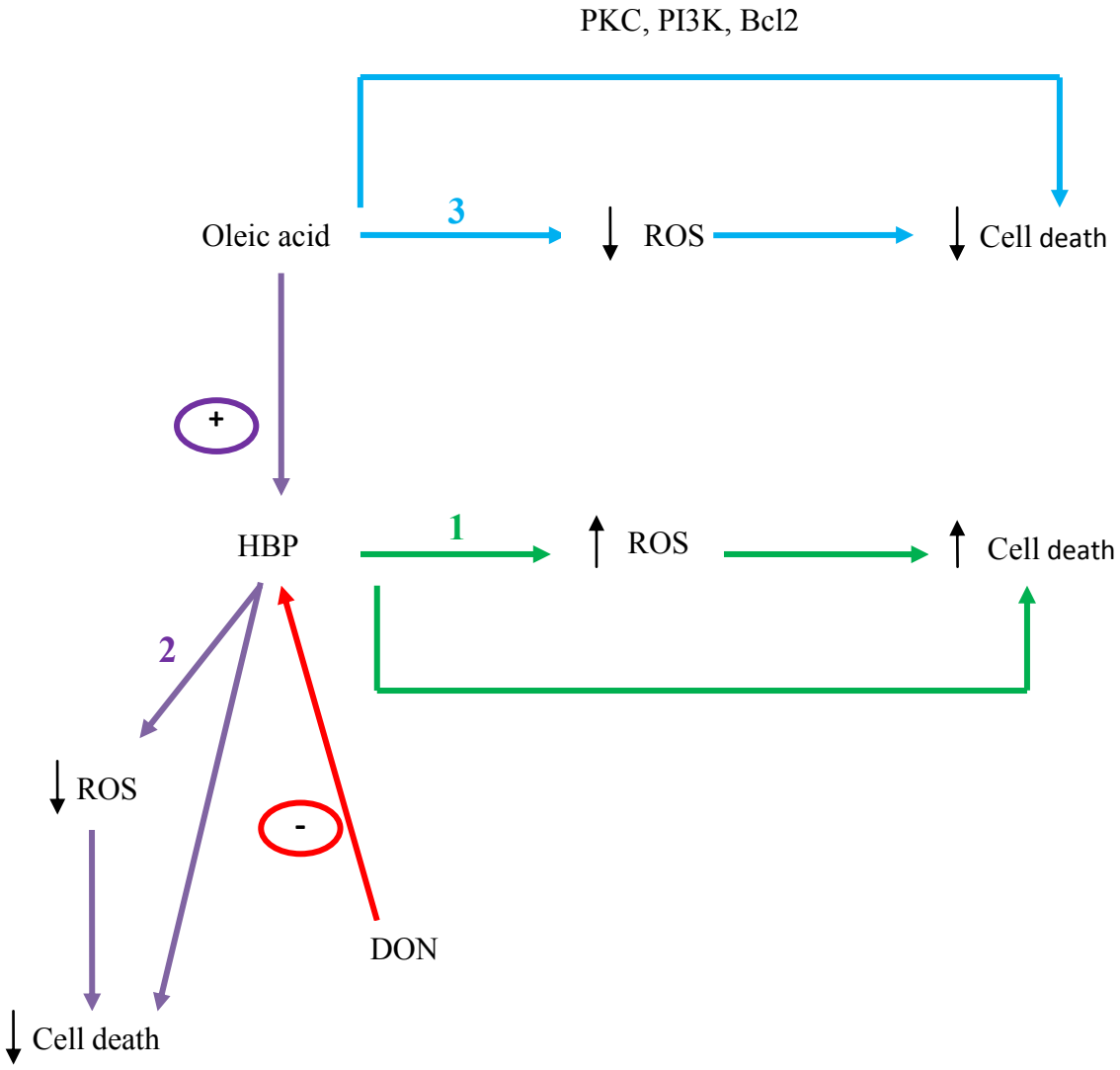

Fig 4.1 Interrelationship between oleic acid and the HBP?

Previous studies found that increased HBP flux may have detrimental or protective effects [1; 14, 15]. Essop et al. (2010) found that higher flux through the HBP caused increased oxidative stress and cell death (apoptosis) [14, 15]. This was shown to occur by increased BAD-*O*-GlcNAcylation and greater BAD-Bcl2 dimerization.

We proposed increased BAD-Bcl2 dimerization, thus causing less Bax-Bcl2 dimerization, greater Bax-Bax dimerization and increased apoptosis.

However, Chatham *et al*. (2010) found that increased *O*-GlcNAcylation contributed to ischemic cardioprotection [1]. An increased *O*-GlcNAylation augmented heat shock protein synthesis (HSP40 and HSP70), both *O*-GlcNAc modified. Increased *O*-GlcNAcylation of transcription factor, Sp1, may contribute to the synthesis of heat shock proteins and the pro-survival of Bcl2 family members. Increased *O*-GlcNAc levels also cause an increase in p38 phosphorylation.

Although p38 is considered to be pro-apoptotic, it can also activate pro-survival pathways through downstream effectors, such as αB-crystallin and HSP27, which both play a role in ischemic protection and are targets of *O*-GlcNAc modification. We believe that our data suggest that pathway #2 (Figure 4.1) is less likely since no additive effects were noted when DON and oleic acid (OA) were combined. Thus, we propose that OA activates the HBP and likely turns on pathway #1 but that this does not form a major part of its action(s).

More likely, it appears to strongly activate pathway #3 to diminish oxidative stress and cell death. Here, cell death may either occur secondarily to the reduction in oxidative stress and/or via direct means, e.g. increased activation of PI3K and/or PKC (Figure 4.1). Increased Bcl2 levels may also contribute to its cardioprotective effects.

4.5 Conclusion

This study explored whether a monounsaturated fatty acid, oleic acid, is able to act as a novel cardioprotective agent. Our *in vitro* data supports this concept and here we show that it is able to blunt oxidative stress and cell death. Moreover, we found that although oleic acid activates the HBP, it does not mediate its protective effects via this pathway alone. Although this study was performed under normoxic conditions, apoptosis is a procedure of programmed cell death that occurs, therefore even though this study was performed under unstressed conditions, the apoptotic data in particular, can be accepted as being statistically and physiologically correct. Moreover, it is part of our future plans to test the efficacy of oleic acid under stressed conditions, e.g. hyperglycemia and/or increased oxidative stress. Therefore further studies in animals and humans are required to confirm our interesting data and to eventually translate this into clinical benefit to patients suffering from diabetes and heart diseases.

4.6 Limitations

It is possible that the technical problems contributed to the lack of changes observed and that our microscopy method requires further optimization. However, the immunoflourescence microscopy data was based on a rather subjective opinion, because the cells that were selected for imaging were the cells that I thought were most representative of the parameter being assessed. For example, in the immunofluorescence microscopy technique, after the four images were taken per well per condition, these images were background subtracted, in order to lessen the amount of fluorescent intensity in the background in order to better view the cells. In my opinion this was unfortunate because in most cases the actual 'true' fluorescence

of the cells were lost, because the level of background subtraction (4 units particularly for my images) had to be maintained for all images, for the purpose of being standard throughout an experiment. In my opinion this led to an under representation of what the fluorescence intensity of the target molecule really was. In cases of the fluorescence intensity already being low, these images in particular were compromised when they were background subtracted.

In my opinion this was the reason for the discrepancy in data when comparing flow cytometry to immunofluorescence microscopy. I do not believe that this had anything to do with my statistical analysis being based on a n=3, since ~60,000 cells were analysed using the flow cytometry technique and 400-800 cells were analysed using immunofluorescence microscopy. Additionally, an n=3 has been used in other publications as well using the same techniques to evaluate certain parameters using H9c2 cells as a experimental model [1, 2].

Another parameter that could also have played a role was the fact that only a single concentration of oleic acid was tested in this study. Our rationale for selecting this particular dosage was based on a previous study that was done using similar techniques, but employing a slightly different experimental model [3]. Thus future work should include a dose-dependent analysis to more fully characterize the effects of oleic acid in our experimental system.

Of note, the term “oxidative stress” was used in a rather loose fashion in this thesis write-up. However, to fully confirm whether this indeed represents ‘’oxidative stress’’, our experimental system should be challenged with varying doses of oleic acid as described above. This is likely to form part of our future studies.

4.7 Future research direction

In order to determine which pathways are involved in the contribution to the beneficial effects of OA in our experimental system we intend to test for OA ± Wortmannin (inhibitor of PI3K) and also OA ± chelerythrine (PKC inhibitor) and if these pathways are blunted and the beneficial effects are lost, this will confirm whether our proposals are indeed correct.

References

Introduction:

1. Aguilar PS, Diegode M. Control of fatty acid desaturation: a mechanism conserved from bacteria to humans. *Molecular Microbiology*. 2006; 62.6: 1507-14.

2. Baron A, Zhu J-S, Zhu J-H, Weldon H, Maianu L, Garvey WT. Glucosamine induces insulin resistance in vivo by affecting GLUT4 translocation in skeletal muscle. *J Clin Invest*. 1995; 96:2792–2801.

3. Bascino H, Federico L, Adeli K. Fructose, insulin resistance, and metabolic dyslipidemia. *Nutrition & Metabolism*. 2005; 2:5.

4. Bethesda, MD. National cholesterol education program: second report of the expert panel on detection, evaluation, and treatment of high blood cholesterol in adults (Adult Treatment Panel II). National Institutes of Health, National Heart, Lung and Blood Institute. 1993; NIH publication No. 93-3095.

5. Brikmann JFF, Abumrad NA, Ibrahimi A, Van der Vusse GJ, Glatz JFC. New insights into long-chain fatty acid uptake by heart muscle: a crucial role of fatty acid translocase/CD36. *Biochem J*. 2002;367:561-570.

6. Brooks G. Intra- and extra-cellular lactate shuttles. *Med Sci Sports Exerc*. 2000; 32:790-799.

7. Buse M. Hexosamines, insulin resistance and the complications of diabetes: current status. *Am J Physiol Endocrinol Metab.* 2006; 290: E1-E8.

8. Chatham JC, Marchase RB. The role of protein O-linked β-N-acetylglucosamine in mediating cardiac stress responses. *Biochim Biophys Acta*. 2010; 1800(2): 57.

9. Chen H, Ing BL, Robinson KA, Feagin AC, Buse MG, Quon MJ. Effects of overexpression of glutamine:fructose-6-phosphate amidotransferase (GFAT) and glucosamine treatment on translocation of GLUT4 in rat adipose cells. *Mol Cell Endocrinol*. 1997; 135:67–77.

10. Chess DJ, Stanley WC. Role of diet and fuel overabundance in the development and progression of heart failure. *Cardiovascular Research.* 2008; 79:269-278.

11. Ciaraldi TP, Carter L, Nikoulina S, Mudaliar S, McClain DA, Henry RR. Glucosamine regulation of glucose metabolism in cultured human skeletal muscle cells: divergent effects on glucose transport/phosphorylation and glycogen synthase in non-diabetic and type 2 diabetic subjects. *Endocrinology*. 1999; 140:3971–3980.

12. Comer F, Hart GW. O-GlcNAc and the control of gene expression. *Biochim Biophys Acta.* 1999; 1473: 161-171.

13. Cook GA. Differences in the sensitivity of carnitine palmitoyltransferase to inhibition of malonyl-CoA are due to differences in Ki-values. *J Biol Chem*. 1984; 259:12030-12033.

14. Coort S, Bonen A, Van der Vusse GJ, Glatz JFF, Luken JJFP. Cardiac substrate uptake and metabolism in obesity and type 2 diabetes: Role of sarcolemmal substrate transporters. *Mol Cell Biol*. 2007;299:5-18.

15. Coort SL, Willems J, Coumans WA, Van der Vusse GJ, Bonen A, Glatz JF, Luiken JJ. Sulfo-N-succinimidyl esters of long chain fatty acids specifically inhibit fatty acid translocase (FAT/CD36)-mediated cellular fatty acid uptake. *Mol Cell Biochem*. 2002; 239:213-219.

16. Covas MI. Olive oil and the cardiovascular system. *Pharmacol Res*. 2007;55:175–86.

17. Davidson KG, Bersten AD, Barr HA, Dowling KD, Nicholas TE, Doyle IR. Lung function, permeability, and surfactant composition in oleic acid-induced acute lung injury in rats. *Am J Physiol Lung Cell Mol Physiol*. 2000; 279:L1091–L1102.

18. Davis RJ. The mitogen-activated protein kinase signal transduction pathway. *J Biol Chem.* 1993; 268:14553–14556.

19. Du X, Mutsumura T, Edelstein D et al. Inhibition of GAPDH activity by poly-(ADP-ribose) polymerase activates three major pathways of hyperglycemic damage in endothelial cells. *J Clin Invest*. 2003; 112(7): 1049-1057.

20. Dyck J, Cheng JF, Stanley WC, Barr R, Chandler MP, Brown S, Wallace D, Arrhenius T, Harmon C, Yang G, Nadzan AM, Lopaschuk GD. Malonyl CoA decarboxylase inhibition protects the ischemic heart by inhibiting fatty acid oxidation and stimulating glucose oxidation. *Circ Res*. 2004; 94: e78-e84.

21. Engelbrecht AM, Engelbrecht P, Genade S, Niesler C, Page C, Smuts M, Lochner A. Long-chain polyunsaturated fatty acids protect the heart against ischemia/reperfusion-induced injury via a MAPK dependent pathway. *J Mol Cell Cardiol*. 2005; 39(6): 940-54.

22. Essop MF, Camp HS, Choi CS, et al. Reduced heart size and increased myocardial fuel substrate oxidation in ACC 2 mutant mice. *Am J Physiol Heart Circ Physiol*. 2008; 295:H256-65.

23. Federici M, Menghini R, Mauriello A, el at. Insulin-dependent activation of endothelial nitric oxide synthase is impaired by O-Linked glycosylation modification of signalling proteins in human coronary endothelial cells. *Circulation*. 2002; 106: 466-72.

24. Frayn KN. The glucose-fatty acid cycle: a physiological perspective. *Biochemical Society Transactions*. 2003; 31:1115-1119.

25. Friedman JM0. A war on obesity, not the obese. *Science*. 2003;299:856–858.

26. Fülöp N, Zhang Z, Marchase RB, Chatham JC. Glucosamine cardioprotection in perfused rat hearts associated with increased O-linked N-acetylglucosamine protein modification and altered p38 activation. Am J Physiol Heart Circ Physiol. 2007; 292(5): H2227-36.

27. Galli C, Calder PC. Effects of fat and fatty acid intake on inflammatory and immune responses: a critical review. *Annuals of nutrition and metabolism.* 2009.

28. Garrison JC, Johnson DE, Campanile CP. Evidence for the role of phosphorylase kinase, protein kinase C and other Ca^{2+}-sensitive protein kinases in the response of hepatocytes to angiotensin II and vasopressin. *J Biol Chem.* 1984;259:3283–3292.

29. Giordano F. Oxygen, oxidative stress, hypoxia, and heart failure. *J Clin Invest*. 2005; 115: 500-508.

30. Gladden L. Lactate metabolism: a new paradigm for the third millennium. *J Physiol*. 2004; 558: 5-30.

31. Greenough, W.B., Crespin, S.R. and Steinberg, D. *Lancet ii*. 1967;1334–1336.

32. Halton TL, Willett WC, Liu S, Manson JE, Albert CM, Rexrode K, Hu FB. Low-carbohydrate-diet score and the risk of coronary heart disease in women. *N Engl J Med.* 2006; 355: 1991–2002.

33. Hawkins M, Angelov I, Liu R, Barzilai N, Rossetti L. The tissue concentration of UDP-N-acetylglucosamine modulates the stimulatory effect of insulin on skeletal muscle glucose uptake. *J Biol Chem.* 1997; 272(8):4889–4895.

34. Hawkins M, Barzilai N, Angelov I, Hu M, Chen W, Rossetti L. The tissue concentration of UDP-N-acetylglucosamine modulates the stimulatory effect of insulin on skeletal muscle glucose uptake. *J Biol Chem*. 1997; 272:4889–4895.

35. Hawkins M, Barzilai N, Chen W, Angelov I, Hu M, Cohen P, Rossetti L. Increased hexosamine availability similarly impairs the action of insulin and IGF-1 on glucose disposal. *Diabetes*1996; 45:1734–1743.

36. Hayashi M, Nasa Y, Tanonaka K, Sasaki H, Miyake R, Hayashi J, Takeo S. The effects of long-term treatment with eicosapentaenoic acid and docosahexaenoic acid on hypoxia/reoxygenation injury of isolated cardiac cells in adult rats. *J Mol Cell Cardiol.* 1995; 27(9): 2013-41.

37. Heart E, Choi WS, Sung CK. Glucosamine-induced insulin resistance in 3T3–L1 adipocytes. *Am J Physiol*. 2000; 278:E103–E112.

38. Hebert L, Daniels M, Zhou J, Crook E, Turner R, Simmons S, Neidigh J, Zhu J-S, Baron A, McClain D. Overexpression of glutamine:fructose-6-phosphate amidotransferase in transgenic mice leads to insulin resistance. *J Clin Invest*. 1996; 98:930–936.

39. Hill JO, Wyatt HR, Reed GW, Peters JC. Obesity and the environment: where do we go from here? *Science*. 2003; 299:853–855.

40. Huang CL, Sumpio BE. Olive oil, the Mediterranean diet, and cardiovascular health. *J Am Coll Surg*. 2008;207:407–16.

41. Jones LG, Ella KM, Bradshaw CD, Gause KC, Dey M, Wisehart-Johnson AE, Spivey EC, Meier KE. Activation of mitogen-activated protein kinases and phospholipase D in A7r5 vascular smooth muscle cells. *J Biol Chem.* 1994; 269:23790–23799.

42. Jossa F, Mancini M. The Mediterranean diet in prevention of arteriosclerosis. *Recenti Prog Med*. 1996; 87:175-181.

43. Kelly T, Yang W, Chen C-S, Reynolds K, He J. Global burden of obesity in 2005 and projections to 2030. *International Journal of Obesity.* 2008; 32:1431-1437.

44. Khan WA, Blobe G, Halpern A, Taylor W, Wetsel WC, Burns D, Loomis C, Hannun YA. Selective regulation of protein kinase C isoenzymes by oleic acid in human platelets. *J Biol Chem.* 1993; 268:5063–5068.

45. Kris-Etherton P, Eckel RH, Howard, BV, St. Jeor S, Bazzarre TL. Lyon diet heart study: benefits of a Mediterranean-style, National cholesterol education program / American Heart Association Step I dietary pattern on cardiovascular disease. *Circulation*. 2001; 103: 1823-1825.

46. Kudo N, Barr AJ, Barr RL, Desai S, Lopaschuk GD. High rates of fatty acid oxidation during reperfusion of ischemic hearts are associated with a decrease in malonyl-CoA levels due to an increase in 5′-AMP-activated protein kinase inhibition of acetyl-CoA carboxylase. *J Biol Chem*. 1995; 270:17513-17520.

47. Lopaschuk G, Folmes CDL, Stanley WC. Cardiac Energy Metabolism in Obesity. *Circ Res*. 2007: 101: 335-347.

48. Lu G, Morinelli TA, Meier KE, Rosenzweig SA, Egan BM. Oleic acid–induced mitogenic signaling in vascular smooth muscle cells: a role for protein kinase C. *Circ Res.* 1996; 79:611–618.

49. Luiken JJ, Koonen DP, Willemse J, Zoranzo A, Becker C, Fischer Y, Tandon NN, Van der Vusse GJ, Bonen A, Glatz JF. Insulin stimulates long-chain fatty acid utilization by

rat cardiac myocytes through cellular redistribution of FAT/CD36. *Diabetes*. 2002; 51:3113-3119.

50. Luiken JJ, Turcotte LP, Bonen A. Protein-mediated palmitate uptake and expression of fatty acid transport proteins in heart giant vesicles. *J Lipid Res*. 1999; 40:1007-1016.

51. Luiken JJFP, Coort SLM, Koonen DPY, Van der Horst DJ, Bonen A, Zorzano A, Glatz JFC. Regulation of cardiac long-chain fatty acid and glucose uptake by translocation of substrate transporters, Pflugers Arch. *Eur J Physiol*. 2004; 448:1-15.

52. Lyle S. Discovering fruit and nuts: A comprehensive guide to cultivation, uses and health benefits of over 300 food-producing plants. Auckland, NZ: David Bateman. 2006.

53. Mackay K, Mochly-Rosen D. Arachidonic acid protects neonatal rat cardiac myocytes from ischaemic injury through epsilon protein kinase C. *Cardiovasc Res*. 2001; 50(1): 65-74.

54. Majane OHI, Vengethasamy L, du Toit EF, Makaula S, Woodiwiss AJ, Norton GR. Dietary-induced obesity hastens the progression from concentric cardiac hypertrophy to pump dysfunction in spontaneously hypertensive rats. *Hypertension.* 2009; 54: 1376–1383.

55. Marshall S, Bacote V, Traxinger RR. Discovery of a metabolic pathway mediating glucose-induced desensitization of the glucose transport system. Role of hexosamine biosynthesis in the induction of insulin resistance. *J Biol Chem*. 1991; 266: 4706-4712.

56. Massaro M, Carluccio MA, De Caterina R. Direct vascular antiatherogenic effects of oleic acid: a clue to the cardioprotective effects of the Mediterranean diet. *Cardiologia*. 1999; 44(6): 507-13.

57. McClain DA, Crook ED. Hexosamines and insulin resistance. *Diabetes*. 1996; 45:1003–1009.

58. McGarry JD, Brown NF. The mitochondrial carnitine palmitoyltransferase system: from concept to molecular analysis. *Eur J Biochem*. 1997; 244:1-14.

59. McGarry JD, Mannaerts GP, Foster DW. A possible role for malonyl-CoA in the regulation of hepatic fatty acid oxidation and ketogenesis. *J Clin Invest*. 1977; 60:265–270.

60. McGarry JD, Mills SE, Long CS, Foster DW. Observations on the affinity of carnitine, and malonyl-CoA sensitivity, of carnitine palmitoyltransferase I in animals and human tissues. Demonstration of the presence of malonyl-CoA in non-hepatic tissues of the rat. *Biochem J*. 1983;214:21-28.

61. Miller TA, LeBrasseur NK, Cote GM, Trucillo MP, Pimentel DR, Ido Y, Ruderman NB, Sawyer DB. Oleate prevents palmitate-induced cytotoxic stress in cardiac myocytes. *Biochem Biophys Res Commun*. 2005; 336(1): 309-15.

62. Moreno JJ, Mitjavila MT. The degree of unsaturation of dietary fatty acids and the development of atherosclerosis [review]. *J Nutr Biochem*. 2003; 14:182–195.

63. Murakami K, Chan SY, Routtenberg A. Protein kinase C activation by cis-fatty acid in the absence of Ca^{2+} and phospholipids. *J Biol Chem.* 1986; 261:15424–15429.

64. Mynatt RL, Lappi MD, Cook GA. Myocardial carnitine palmitoyltransferas of the mitochondrial outer membrane is not altered by fasting. *Biochim Biophys Acta*. 1992; 1128:105-111.

65. Onay-Besikci A, Campbell FM, Hopkins TA, Dyck JR, Lopaschuk GD. Relative importance of malonyl-CoA and carnitine in maturation of fatty acid oxidation in new born rabbit heart. *Am J Physiol Heart Circ Physiol*. 2003; 284: H283-H289.

66. Opie LH. Heart Physiology from cell to circulation. 4th edition. Philadelphia, PA: Lippincott Williams & Wilkins; 2004.

67. Panagiotakos DB, Dimakopoulou K, Katsouyanni K, Bellander T, Grau M, Koenig W, Lanki T, Pistelli R, Schneider A, Peters A. Mediterranean diet and inflammatroy response in myocardial infarction survivors. *Int J Epidemiology*. 2009; 38:856-866.

68. Paton CM, Ntambi JM. Biochemical and physiological function of stearoyl-CoA desatuarse. *Am J Physiol Endocrinol Metab*. 2009; 297(1):E28-37.

69. Patti ME, Virkamaki A, Landaker EJ, Kahn CR, Yki-Jarvinen H. Activation of the hexosamine pathway by glucosamine in vivo induces insulin resistance of early postreceptor insulin signaling events in skeletal muscle. *Diabetes*. 1999; 48:1562–1571.

70. Penny S. Food matters: A guide to healthy eating & supplements. Wellington, NZ: Massey University, Institute of food, nutrition and human health. 2004.

71. Pitout V, Hagman D, Stein R, Artner I, Robertson RP, Harmon JS. Regulation of the insulin gene by glucose and fatty acids. *J of Nutr*. 2006; 136: 873-876.

72. Pohl J, Ring A, Hermann T, Stremmel W. Role of FATP in parenchymal cell fatty acid uptake. *Biochim Biophys Acta*. 2004; 1686:1-6.

73. Rajamani U, Essop MF. Hyperglycemia-mediated activation of the hexosamine biosynthetic pathway results in myocardial apoptosis. *Am J Physiol Cell Physiol*. 2010; 299: C139-C147.

74. Rajamani U, Joseph D, Roux S, Essop MF. The hexosamine biosynthetic pathway can mediate myocardial apoptosis in a rat model of diet-induced insulin resistance. *Acta Physiol*. 2011; 202: 151-157.

75. Randle PJ, Garland PB, Hales CN, Newsholme EA. *Lancet i*. 1963; 785–789.

76. Randle PJ. Regulatory interactions between lipids and carbohydrates: the glucose fatty acid cycle after 35 years. *Diabete Metab* 1998; Rev14:263 –283.

77. Ravussin E. Cellular sensors of feast and famine. *J Clin Invest*. 2002; 109: 1537-1540.

78. Robinson K, Weinstein ML, Lindenmayer GE, Buse MG. Effects of diabetic and hyperglycemia on the hexosamine synthesis pathway in rat muscle and liver. *Diabetes*. 1995; 44: 1438-14456.

79. Robinson KA, Sens DA, Buse MG. Pre-exposure to glucosamine induces insulin resistance of glucose transport and glycogen synthesis in isolated rat skeletal muscles. *Diabetes*. 1993; 42:1333–1346.

80. Rossetti L, Giaccari A, DeFronzo RA. Glucose toxicity. *Diabetes Care*. 1990; 13:610-630.

81. Rossetti L, Hawkins M, Chen W, Gindi J, Barzilai N. *In vivo* glucosamine infusion induces insulin resistance in normoglycemic but not in hyperglycemic conscious rats. *J Clin Invest*. 1995; 96:132–140.

82. Saddik M, Gamble J, Witters LA, Lopaschuk GD. Acetyl-CoA carboxylase regulation of fatty acid oxidation in the heart. *J Biol Chem*. 1993; 268: 25836-25845.

83. Saha AK, Kurowski TG, Ruderman NB. A malonyl-CoA fuel-sensing mechanism in muscle: effects of insulin, glucose, and denervation. *Am J Physiol*. 1995; 269:E283–E289.

84. Schelling P, Fischer H, Ganten D. Angiotensin and cell growth: a link to cardiovascular hypertrophy? *J Hypertens*. 1991;9:3–15.

85. Schwrtz MW, Woods SC, Porte D Jnr, Seeley RJ, Baskin DG. Central nervous system control of food intake. *Nature*. 2000; 404:661-671.

86. Seyffert, Jr, W.A. and Madison, L.L. *Diabetes*. 1967;16:765–776.

87. Silverthorn DU. Human physiology: a integrated approach. 4th edition. San Francisco, CA: Benjamin Cummings; 2007.

88. Stanley W, Morgan EE, Huang H, McElfresh TA, Strek JP, Okere IC, Chandler MP, Cheng J, Dyck JRB, Lopaschuk GD. Malonyl-CoA decarboxylase inhibition suppresses fatty acid oxidation and reduces lactate production during demand-induced ischemia. *Am J Physiol Heart Circ Physiol*. 2005; 289: H2304-H2309.

89. Stanley WC, Recchia FA, Lopaschuk GD. Myocardial substrate metabolism in the normal and failing heart. *Physiol Rev*. 2005; 85: 1093-1129.

90. Stryler L. Biochemistry. 4th edition. New York: Freeman and Company. 1999; 483-628.

91. Taegtmeyer H, McNuty P, Young ME. Adaptation and maladaptation of the heart in diabetes: Part I. General concepts. *Circulation*. 2002; 105: 1727-1733.

92. Ternus ME, Lapsley K, Geiger CJ. Health benefits of tree nuts. 2009.

93. Traxinger RR, Marshall S. Coordinated regulation of glutamine:fructose-6-phosphate amidotransferase activity by insulin, glucose, and glutamine. *J Biol Chem.* 1991; 266 (16):10148–10154.

94. Tsimikas S, Phillis-Tsimikas A, Alexopoulos S, Sigari F, Lee C, Reaven PD. LDL isolated from Greek subjects on a typical diet or from American subjects on an oleate-supplemented diet induces less monocyte chemotaxis and adhesion when exposed to oxidative stress. *Arterioscler Thromb Vasc Biol*. 1999; 19:122-130.

95. Vadász I, Morty RE, Kohstall MG, Olschewski A, Grimminger F, Seeger W, Ghofrani HA. Oleic acid inhibits alveolar fluid reabsorption: a role in acute respiratory distress syndrome? *Am J Respir Crit Care Med*. 2005; 171:469–479.

96. Walker C, Reamy BV. Diets for cardiovascular disease prevention: what is the evidence? *Am Fam Physician*. *2009*; *79:571*–8.

97. Wang LY, Ma JK, Pan WF, Toledo-Velasquez D, Malanga CJ, Rojanasakul Y. Alveolar permeability enhancement by oleic acid and related fatty acids: evidence for a calcium-dependent mechanism. *Pharm Res*. 1994; 11:513–517.

98. Wells L, Gao Y, Mahoney JA, Vosseller K, Chen C, Rosen A, Hart GW. J Biol Chem. 2002; 277: 1755-1761.

99. Wild S, Roglic G, Green A, Sicree R, King H. Global prevalence of Diabetes: Estimates for the year 2000 and projections for 2030. *Diabetes Care*. 2004;27:1047-1053.

100. Wisneski JA, Gertz EW, Neese RA, Mayr M. Myocardial metabolism of free fatty acids: studies in 14C-labeled substrates in humans. *J Clin Invest*. 1987; 79: 359-366.

101. Young M, Goodwin GW, Ying J, Guthrie P, Wilson CR, Laws FA, Taegtmeyer H. Regulation of cardiac and skeletal muscle malonyl-CoA decarboxylase by fatty acids. *Am J Physiol Endocrinol Metab*. 2001; 280: E471-E479.

102. Zachara N, Hart GW. Cell signalling, the essential role of O-GlcNAc! *Biochim Biophys Acta*. 2006; 1761: 599-617.

Materials and Methods:

1. Hescheler J, Meyer R, Plant S, Krautwurst D, Rosenthal W, Schultz G. Morphological, biochemical, and electrophysiological characterization of a clonal cell (H9c2) line from rat heart. *Circ Res*. 1991; 69: 1476-1486.

2. Kimes BW, Brandt BL. Properties of a clonal muscle cell line from rat heart. *Exp Cell Res*. 1976; 98: 367-381.

3. Lagranha CJ, et al. Glutamine enhances glucose-induced mesangial cell proliferation. *Amino acids*. 2008; 34(4):683-5.

4. Sipdo KR, Marban E. L-type calcium channels, potassium channels and novel nonspecific cation channels in a clonal muscle cell line derived from embryonic rat ventricle. *Circulation research*. 1991; 69:6

5. Van der Lee KAJM, Vork MM, De Vries JE, Willemsen PHM, Glatz JFC, Reneman RS, Van der Vusse GJ, Van Bilsen M. Long-chain fatty acid-induced changes in gene expression in neonatal cardiac myocytes. *Journal of Lipid Res*. 2000; 41: 41-47.

Discussion:

1. Chatham JC, Marchase RB. The role of protein O-linked β-N-acetylglucosamine in mediating cardiac stress responses. *Biochim Biophys Acta*. 2010; 1800(2): 57.

2. De Vries JE, Vork MM, Roemen thm, De JongYF, Cleutjens JPM, Van der Musse GJ, Van Bilsen M. Saturated but not mono-unsaturated fatty acids induce apoptotic cell death in neonatal rat ventricular myocytes. *J of Lip Res*. 1997; 38:1384-1394.

3. Ghosh, Rodrigues B. Cardiac cell death in early diabetes and its modulation by dietary fatty acids. *Biochimica et Biophysica Acta*. 2006; 1761: 1148-1162.

4. Hardy S, Langelier Y, Prentki M. Oleate activates phosphatidylinositol 3-kinase and promotes proliferation and reduces apoptosis of MDA-MB-231 breast cancer cells, whereas palmitate has opposite effects. *Cancer Res*. 2000; 60(22):6353-8.

5. Huertas JR, Battino M, Mataix FJ, Lenaz G. Changes in mitochondrial and microsomal Q_9 and Q_{10} content induced by dietary fat and endogenous lipid peroxidation. *FEBS Lett*. 1991; 287: 89-92.

6. Kris-Etherton P, Eckel RH, Howard, BV, St. Jeor S, Bazzarre TL. Lyon diet heart study: benefits of a Mediterranean-style, National cholesterol education program / American Heart Association Step I dietary pattern on cardiovascular disease. *Circulation*. 2001; 103: 1823-1825.

7. Maedler K, Oberholzer J, Bucher P, Spinas GA, Donath MY. Monounsaturated fatty acids prevent the deleterious effects of palmitate and high glucose on human pancreatic β-cell turnover and function. *Diabetes*. 2003; 52:726-733.

8. Narang D, Sood S, Thomas M, Dinda AK, Maulik SK. Dietary palm olein oil auguments cardiac antioxidant enzymes and protects against isoproterenol-induced myocardial necrosis in rats. *J Pharm Pharmacol*. 2005; 57(11): 1445-51.

9. Narang D, Sood S, Thomas MK, Dinda AK, Maulik SK. Effect of dietary palm olein oil on oxidative stress associated with ischemic-reperfusion injury in isolated rat heart. *BMC Pharmacol*. 2004; 4:29.

10. Ochoa-Herrera JJ, Huertas JR, Quiles JL, Mataix J. Dietary oils high in oleic acid, bur with different non-glyceride contents, have different effects on lipid profiles and peroxidation in rabbit hepatic mitochondria. *J Nutr Biochem*. 2001; 12: 257-264.

11. Oudit GY, Sun H, Kerfany BG, Crackower MA, Penninger JM, Backx PH. The role of phosphoinositide-3 kinase and PTEN in cardiovascular physiology and disease. *J Mol Cell Cardiol.* 2004; 37(2): 449-71.

12. Quiles JL, Barja G, Battino M, Mataix J, Solfrizzi V. Role of olive oil and monounsaturated fatty acids in mitochondrial oxidative stress and aging. *Nutrition Reviews*. 2006; 64:10.

13. Quiles JL, Huertas JR, Manas M, Battino M, Mataix J. Physical exercise affects the lipid profile of mitochondrial membranes in rats fed with virgin olive oil or sunflower oil. *Br J Nutr*. 1999; 81: 21-24.

14. Rajamani U, Essop MF. Hyperglycemia-mediated activation of the hexosamine biosynthetic pathway results in myocardial apoptosis. *Am J Physiol Cell Physiol*. 2010; 299: C139-C147.

15. Rajamani U, Joseph D, Roux S, Essop MF. The hexosamine biosynthetic pathway can mediate myocardial apoptosis in a rat model of diet-induced insulin resistance. *Acta Physiol*. 2011; 202: 151-157.

16. Singh JK, Dasgupta A, Adayev T, Shahmehdi SA, Hammond D, Banerjee P. Apoptosis is associated with an increase in saturated fatty acid-containing phospholipids in the neuronal cell line. *Biochim Biophys Acta.* 1996; 1304: 171-178.

17. Surette ME, Winkler JD, Fonteh AN, Chilton FH. Relationship between arachidonate-phospholipid remodelling and apoptosis. *Biochemistry*. 1996; 35: 9187-9196.

Limitations:

1.Mukhopadhyay P, Rajesh M, Yoshihiro K, Hasko G, Pacher P. Simple quantitative detection of mitochondrial superoxide production in live cells. *Biochem Biophy Res Commun*..2007; 358(1):203-208.

2. Mutharasan RK, Nagpal V, Ichikawa Y, Ardehali H. MicroRNA-210 is upregulated in hypoxic cardiomyocytes through Akt- and p53-dependent pathways and exerts cytoprotective effects. *Am J Physiol Heart Circ Physiol*. 2011; 301:H1519-H1530.

3. Van der Lee KAJM, Vork MM, De Vries JE, Willemsen PHM, Glatz JFC, Reneman RS, Van der Vusse GJ, Van Bilsen M. Long-chain fatty acid-induced changes in gene expression in neonatal cardiac myocytes. *Journal of Lipid Res*. 2000; 41: 41-47.